HHS Public Access

Author manuscript

Int J Pharm. Author manuscript; available in PMC 2022 January 25.

Published in final edited form as:

Int J Pharm. 2021 January 25; 593: 120121. doi:10.1016/j.ijpharm.2020.120121.

Development of a formulation platform for a spray-dried, inhalable tuberculosis vaccine candidate

Mellissa Gomez[1], **Joseph McCollum**[2], **Hui Wang**[1], **Mani Ordoubadi**[1], **Chester Jar**[1], **Nicholas B. Carrigy**[1], **David Barona**[1], **Isobel Tetreau**[1], **Michelle Archer**[2], **Alana Gerhardt**[2], **Chris Press**[2], **Christopher B. Fox**[2,3], **Ryan M. Kramer**[2], **Reinhard Vehring**[1]

[1]Department of Mechanical Engineering, University of Alberta, Edmonton, AB, Canada

[2]Infectious Disease Research Institute, Seattle, WA, USA

[3]Department of Global Health, University of Washington, Seattle, WA, USA

Abstract

Protection against primarily respiratory infectious diseases, such as tuberculosis (TB), can likely be enhanced through mucosal immunization induced by direct delivery of vaccines to the nose or lungs. A thermostable inhalable dry powder vaccine offers further advantages, such as independence from the cold chain. In this study, we investigate the formulation for a stable, inhalable dry powder version of an adjuvanted subunit TB vaccine candidate ID93+GLA-SE, containing recombinant fusion protein ID93 and glucopyranosyl lipid A (GLA) in a squalene emulsion (SE) as an adjuvant system, via spray drying. The addition of leucine (20% w/w), pullulan (10%, 20% w/w), and trileucine (3%, 6% w/w) as dispersibility enhancers was investigated with trehalose as a stabilizing agent. Particle morphology and solid state, nanoemulsion droplet size, squalene and GLA content, ID93 presence, and aerosol performance were assessed for each formulation. The results showed that the addition of leucine improved aerosol performance, but increased aggregation of the emulsion droplets was demonstrated on reconstitution. Addition of pullulan preserved emulsion droplet size; however, the antigen could

Corresponding Author: R. Vehring, University of Alberta, 116 St & 85 Ave, Edmonton Canada, reinhard.vehring@ualberta.ca.

Mellissa Gomez – Conceptualization, Methodology, Formal analysis, Investigation, Visualization, Writing – Original Draft, Writing – Review & Editing
Joseph McCollum – Methodology, Formal Analysis, Investigation, Writing – Review & Editing
Hui Wang – Conceptualization, Methodology, Investigation, Writing - review & editing
Mani Ordoubadi – Conceptualization, Methodology, Software, Visualization, Writing – Review & Editing
Chester Jar – Formal analysis, Investigation, Visualization, Writing – Review & Editing
Nicholas B. Carrigy – Conceptualization, Methodology, Resources, Writing – Review & Editing
David Barona – Conceptualization, Resources, Writing – Review & Editing
Isobel Tetreau – Formal analysis, Investigation, Visualization, Writing – Review & Editing
Michelle Archer – Methodology, Writing – Review & Editing
Alana Gerhardt – Supervision, Writing – Review & Editing
Chris Press – Methodology, Formal analysis, Investigation, Writing – Review & Editing
Christopher B. Fox – Conceptualization, Funding acquisition, Project administration, Writing – Review & Editing
Ryan M. Kranter – Conceptualization, Project administration, Supervision, Writing – Review & Editing
Reinhard Vehring – Conceptualization, Formal analysis, Funding acquisition, Methodology, Project administration, Supervision, Writing – Review & Editing

not be detected after reconstitution. The trehalose-trileucine excipient formulations successfully stabilized the adjuvant system, with evidence indicating retention of the antigen, in an inhalable dry powder format suitable for lung delivery.

Graphical Abstract

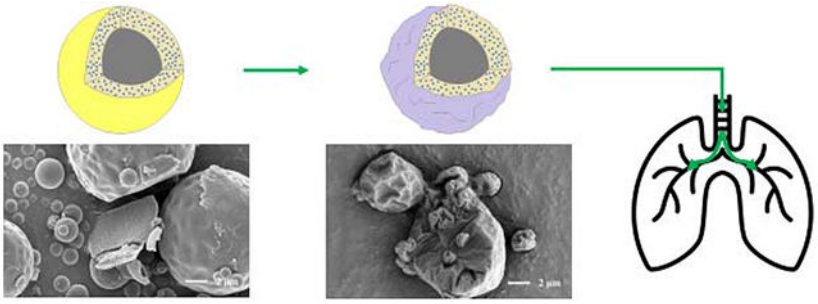

Keywords

spray drying; tuberculosis vaccine; inhalable delivery; nanoencapsulation; particle engineering; dispersibility

1 Introduction

Spray drying is a method of desiccating a liquid product into a dry powder composed of many small particles. Briefly, a liquid feedstock is atomized into small droplets during spray drying. These droplets, containing dissolved or suspended solids, evaporate within a drying gas into particles. The particles are then separated from the flow, e.g. with a cyclone. Spray drying is commonly used in the food processing and pharmaceutical industries to encapsulate an active component into a dry powder and thus protect it from potentially harmful environmental conditions, such as high humidity and temperature [1]. Spray drying has been previously used to improve the stability of experimental vaccines using the disaccharide trehalose as a stabilizer [2, 3, 4, 5]. Spray drying also allows for engineering of the resulting particles for specific properties, making them suitable for intranasal or pulmonary routes via inhalation [6, 7, 8]. Both the improvement of thermostability and the development of an inhalable route of delivery may be applied to vaccines to improve their accessibility.

Preclinical trials of dry powder vaccines have been promising. However, as dry powder vaccination via inhalation is an emerging field, clinical trials are limited. The first inhalable dry powder vaccine for pulmonary delivery, a measles vaccine, completed Phase I clinical trials in 2013 [9]. Further work is warranted because there are many benefits to developing alternative administration routes to injection. The general advantages of respiratory drug delivery include convenience, reduced chance of adverse systemic reactions, and smaller amounts of drug required due to direct targeting. Compared to injectable delivery, the use of a non-invasive route of administration reduces the chance of needlestick injuries, and with that reduces the transmission of blood-borne illnesses such as HIV. Additionally, injectable delivery of a reconstituted vaccine requires sterile water, a commodity that is taken for

granted in developed nations. Furthermore, mucosal immunization through inhalable delivery is potentially more effective at conferring protection than parenteral injection against respirable diseases, such as tuberculosis (TB) [10].

TB is the leading cause of death from a single infectious agent, and approximately 10 million people contracted TB in 2018 [11]. TB is transmitted through air as droplets, making the lungs the primary infection site [12]. Currently, the bacille Calmette-Guerin (BCG) vaccine is the only licensed TB vaccine. BCG is administered via injection as part of standard childhood immunization programs in many countries [11]. Due to the widespread use of BCG, any improvement in efficacy would have a large impact. To this end, administration routes alternative to injection have been investigated for BCG. Research involving animal models have reported that the BCG vaccine provides better protection against TB when administered to the respiratory system directly rather than through injection [13, 14, 10, 15]. Aguilo et al. [10] demonstrated that intranasal delivery of BCG, but not subcutaneous delivery, conferred protection against pulmonary TB in TB-susceptible mice. Verreck et al. [15] suggested that pulmonary immunization results in a more reliably protective local immune response. Recently, Price et al. [6] spray-dried the BCG vaccine into a thermostable presentation designed for inhalable dry powder delivery. Mouse immunization studies showed that the liquid BCG vaccine, the reconstituted freshly spray-dried BCG vaccine, and the reconstituted spray-dried BCG vaccine stored at 25 °C for two years had no significant difference in induced cytokine response in mice. However, despite the effort in improving the efficacy of BCG vaccine via different routes of delivery, the vaccine carries several limitations. It has demonstrated variable efficacy in humans based on geography (0-80%) [16], confers only limited protection to adults [11], is unsafe for immunocompromised infants [17], and is not effective in preventing latent TB from becoming active [11]. Alternative vaccines for TB are being developed to address these shortcomings.

One such vaccine candidate is ID93+GLA-SE, an adjuvanted subunit vaccine comprised of a recombinant fusion antigen, ID93, and an adjuvant system, GLA-SE. The main components of the adjuvant system consist of synthetic TLR4 agonist glucopyranosyl lipid A (GLA), squalene nanodroplets, and DMPC as an emulsifier. ID93+GLA-SE has shown promising results in animal models [18] and has progressed to Phase II clinical testing [11]. Conversion of this vaccine to a thermostable presentation has been explored, as per WHO guidelines, to focus on thermostable options for promising candidates [19, 20]. Both lyophilization [21, 22] and spray drying [23] have been investigated as desiccation methods and were found to confer thermostability to ID93+GLA-SE. The lyophilized vaccine candidate is currently undergoing a Phase I clinical trial [24]. Spray drying was investigated as an alternative method as it is considered more scalable than lyophilization, potentially has lower processing costs [25, 26], and also allows for the manipulation of morphology and structure of the final particle product. Previous work spray-drying ID93+GLA-SE focused on the development and stability of a presentation designed for eventual reconstitution and injection that utilized only trehalose as a stabilizing excipient [23]. The promising results demonstrated by the spray-dried presentation prompted investigation into spray drying an inhalable presentation of ID93+GLA-SE.

Respiratory delivery of an aerosolized powder occurs through nasal or pulmonary routes, each with an optimum particle size range for the most effective drug delivery. Drug particles or drug sprays are usually delivered locally during nasal administration, whereas the active components for pulmonary delivery must surpass the upper extrathoracic airways before it can deposit in either the targeted trachea-bronchia region or the targeted alveolar region [27]. Therefore, successful pulmonary delivery requires smaller particles (1-5 μm) than for nasal delivery (~20 μm) and much more flowable drug particles that need to be carefully designed [28, 29, 30, 31]. In addition, to achieve successful lung deposition, particles must also not get stuck in the delivery device, or be exhaled out. Therefore, the formulation development for pulmonary delivery can be much more challenging. Two of the most important factors that need to be considered during dry powder formulation development are the aerodynamic particle size and dispersibility of the powder [32]. However, delivery devices, such as dry powder inhalers (DPI), are usually unable to fully disperse the powder due to the intrinsic cohesiveness of the powder. The addition of larger carrier particles is a traditional method to reduce powder retention within DPIs. However, added carriers should be used only for potent actives as they reduce the drug load per inhaled dose. Instead, particle engineering can be used to improve powder dispersibility through the addition of dispersibility enhancing agents such as leucine, pullulan, and trileucine.

Leucine is an amino acid that has been proposed in combination with trehalose as a system to stabilize biologics [33]. The leucine component of spray-dried formulations has been designed to form a fully crystalline, rugose outer shell to improve the dispersibility of a powder [34, 35]. Pullulan is a polysaccharide that has been used in the food drying industry and pharmaceutical industry to improve thermostability. Films formed from drying pullulan with trehalose have been reported to improve the thermostability of live-attenuated or inactivated viral vaccines for up to 12 weeks at 40 °C [36]. Under normal spray drying conditions, both pullulan and trehalose remain amorphous [37]. Trileucine is a tripeptide that has been shown to form an amorphous layer on spray-dried particles under normal spray drying conditions [38]. The formation of a trileucine layer has been shown to reduce particle cohesiveness and thus improve aerosol performance [39]. The addition of trileucine has also been shown to improve the stability of trehalose microparticles suspended in HFA227ea propellant [40] and the stability of spray-dried bacteriophages [41].

Improved thermostability and development of an inhalable route would be especially beneficial for intervention of TB. This paper studies three dispersibility enhancers: leucine, pullulan and trileucine, for producing spray-dried ID93+GLA-SE powder suitable for inhalation. Success of the inhalable candidates was assessed in terms of aerosol performance and preservation of vaccine integrity after spray drying. Characterization of vaccine integrity included testing for changes in emulsion size distribution, squalene and GLA content, and presence of ID93.

2 Materials and Methods

2.1 Materials

Chemicals—Trehalose dihydrate with a purity of 98% was used as the primary stabilizing excipient for spray drying (CAS 6138-23-4; Fisher Scientific Ottawa, ON, Canada). L-

Leucine with a purity of 99% (CAS 61-90-5; Fisher Scientific Ottawa, ON, Canada), pullulan (CAS 9057-02-7; Alfa Aesar, Tewksbury, MA, USA), and trileucine with a purity of ≥90% (CAS 10329-75-6; Sigma Aldrich, Oakville, ON, Canada) were investigated as dispersibility enhancing materials. Tris(hydroxymethyl)aminomethane (Tris) (CAS 77-86-1; Sigma Aldrich, Oakville, ON, Canada) and hydrochloric acid (CAS 7647-01-0; Sigma Aldrich, Oakville, ON, Canada) were used as a buffer system to adjust the pH of the feedstock prior to spray drying. Formulations were made using HPLC grade water (CAS 7732-18-5; Fisher Scientific Ottawa, ON, Canada) or deionized water. The ID93 antigen and GLA-SE adjuvant system were formulated separately; manufacturing of these components has been described elsewhere [23].

Formulation Composition—Six formulations were assessed as inhalable vaccine candidates. The feedstock composition and the projected material composition of the final dried particles are given in Table 1. Concentrations for several of the main components, including trehalose, GLA-SE, ID93, and Tris buffer, were kept constant for all the formulated liquid feedstocks, as listed in the table.

ID93 protein was stored at a concentration of 1.2 mg/mL at −80 °C prior to use. GLA-SE nanoemulsions with a squalene concentration of 10% v/v and GLA concentration of 50 μg/mL were stored in a refrigerator prior to use. All formulation processes began with preparation of 4 mg/ml Tris. The Tris solution was then pH adjusted by addition of hydrochloric acid to a pH of 7.5±0.1. Preliminary work found that the buffer system had no apparent effect on particle morphology. For each formulation, the trehalose and relevant dispersibility enhancing agent were dissolved in water into buffered Tris solution. Once fully dissolved, GLA-SE was added and the solution gently mixed. ID93 was added last to the feedstock to minimize potential protein binding to container surfaces.

Previous work [23] found that a high encapsulation efficiency of the vaccine candidate was achieved by spray drying 4 μg/mL of ID93, 10 μg/mL of GLA, and 17.2 mg/mL of squalene with 100 mg/ml of trehalose. The same ratios of excipient, antigen, and adjuvant system were kept in this work to target a high encapsulation efficiency. The correct antigen and adjuvant concentration for an inhalable route of administration has not been determined and may need to be increased in the future.

2.2 Spray Drying

Spray drying parameters were chosen in order to minimize potential antigen or agonist losses during processing based on a previous study involving spray drying ID93+GLA-SE [23]. A custom research spray dryer [42] with a twin fluid atomizer was utilized to conduct the spray drying. Use of a twin-fluid atomizer has been reported to significantly reduce degradation of a shear- and temperature-sensitive protein during the atomization step as compared to use of a vibrating mesh atomizer [43, 44]. The atomizer was operated at an air-liquid ratio of 8, corresponding to a mass median initial droplet diameter of approximately 9 μm. Characterization of the atomizer is described elsewhere [45].

A relatively low drying gas temperature of 65 °C was utilized in order to minimize temperature-dependent degradation. The other spray drying parameters were calculated

using an energy and balance model [46] to achieve an outlet humidity of less than 10% relative humidity and low outlet temperature. A low outlet humidity was targeted to achieve a low (2-3%) powder moisture content as over-drying can also lead to protein degradation. A low outlet temperature was chosen to limit the temperature the powder was exposed to during cyclone collection. The feedstock was supplied to the atomizer at a rate of 0.6 mL/min using a peristaltic pump (Model 77200-60; Cole-Parmer, Montreal, QC, Canada), and the drying gas flow rate was set to 200 SLPM, leading to a low outlet temperature of approximately 36 °C. Powders were stored under dry conditions prior to characterization.

2.3 Particle Design

Respirable Range—The target particle aerodynamic diameter range for this study was chosen to be 3-4 μm. The range in feedstock concentration to produce particles within the target size range was calculated using Eq. 1, where, d_a, is the aerodynamic diameter, ρ_P is the particle density, ρ^* is the reference density (1000 kg/m^3), c_F is the feedstock concentration, and d_D is the diameter of the droplets [38]. Further details on the derivation of this equation can be found elsewhere [38].

$$d_a = \sqrt[6]{\frac{\rho_P}{\rho^*}}\sqrt[3]{\frac{c_F}{\rho^*}}d_D \quad (1)$$

Previous work has shown that spray drying the ID93+GLA-SE vaccine produces particles with varying shell thicknesses [23]. Material density of this formulation was estimated to be 1438 kg/m^3. Previous studies on spray drying of emulsions [47, 48] and spray drying formulations containing leucine [34] have shown that the resulting particles are hollow, with varying degrees of shell thicknesses. Spray drying of formulations containing trileucine have been shown to produce particles with external void space [39]. Based on these findings, preliminary calculations assumed that the average particle in this study contained approximately 30% void space. Therefore, the particle density can be roughly approximated to be 1000 kg/m^3. Initial droplet diameter was predicted to be 9 μm based on the processing conditions. Based on these assumptions, the concentration of the feedstock must be between 37 and 88 mg/mL to achieve a particle size between 3 and 4 μm.

Selection of Excipients to Improve Powder Dispersibility—Aerodynamic particle size is a strong indicator of a powder's ability to deposit within the lung. Therefore, dispersing particle aggregates into primary particles is essential; otherwise, aggregated small particles will behave aerodynamically as larger particles and potentially deposit prior to the lung. However, passive delivery devices, such as DPIs, can only provide limited dispersing force as they rely soley on the patients' inhalation flow to de-aggregate the loaded powder dosages. Thus, it is necessary to reduce intrinsic powder cohesiveness to improve the dispersibility. Powder cohesiveness can be described in terms of the contact mechanics between adjacent particles. Based on theoretical cohesion models, e.g. the Li-DMT model [49], the force of cohesion between two particles, F_c, can be reduced by lowering the surface energy, decreasing the deformability of the surface, and decreasing the contact area.

The excipients investigated in this study, leucine, pullulan, and trileucine, were expected to reduce the force of cohesion between particles. The component mass fraction for all investigated dispersibility enhancing agents in this study was limited to a maximum of 20% in order to maximize the adjuvant dose in the powder. Leucine was chosen as it has been reported to change the surface morphology of spray-dried particles through formation of a crystalline surface layer. Increasing leucine concentration changes particle surface from a smooth morphology to solid particles with corrugated surfaces [34, 35]. Additional increases in leucine concentration further changes particle morphology to rugose hollow particles. The increased surface roughness due to crystal surface asperities is expected to reduce effective contact area between particles. Additionally, the formation of a crystalline outer layer is expected to reduce the deformability of the surface as compared to an amorphous particle surface. Feng et al. [34] reported that, for their given spray drying parameters, 25% leucine mass fraction in a leucine-trehalose system was required to achieve complete crystallinity of leucine. Thus, a mass fraction of 20% leucine was chosen for the T20Leu formulation to promote crystal growth in order to improve powder dispersibility.

Pullulan was chosen as it has been shown to introduce particle folding in pullulan-trehalose systems [37]. The change in surface morphology may decrease effective contact area, depending on particle orientation. Carrigy et al. [37] reported that the formation of folded, irregularly shaped particles increases with increasing pullulan concentration, and 10% pullulan mass fraction in a pullulan-trehalose system slightly improved aerosol performance as compared to a trehalose-only formulation. Based on these results, a mass fraction of 10% pullulan was chosen for the T10Pul formulation in order to modify the surface morphology to promote improved dispersibility. Due to the reported increase in particle folding with increased pullulan content, a mass fraction of 20% pullulan for the T20Pul formulation was also investigated.

Trileucine was chosen as it has been reported to form highly wrinkled particle surfaces with increasing concentration, and has been shown to decrease the surface energy of spray-dried particles [39, 40]. Highly rugose particle surface morphologies are expected to decrease contact area between particles, and reduced surface energy is expected to reduce the force of cohesion between particles. Wang et al. [40] demonstrated that at 1.0% mass fraction of trileucine in trileucine-trehalose systems the particle morphology appears rugose. Particle surface rugosity was improved greatly when the trileucine mass fraction was increased to 5.0%. Due to trileucine solubility limitations, 6% trileucine by mass for the T6Tri formulation was chosen for investigation in this study. 6%, a relatively high mass fraction, was chosen in order to promote increased particle surface rugosity and thus reduce particle cohesion. A lower mass fraction of 3% for the T3Tri formulation was also investigated in this study to determine if a similar performance could be obtained with a formulation with lower excipient costs.

Particle Formation Model—Previous studies have reported the mass fractions of leucine, pullulan, and trileucine required to induce surface morphology changes. However, these studies utilized different spray drying processing conditions. Change in processing conditions will affect the distribution of components within a drying droplet. A simple particle formation model [50] was used to predict drying time and component distribution of

the investigated formulations to verify that the dispersibility agents will form a shell on the particle exterior for the given spray drying parameters.

As the droplet dries, the radial concentration gradient of the formulation components is controlled by two mechanisms: the receding droplet surface and the diffusion of solutes from the surface towards the center of the droplet [50, 51]. The former mechanism will increase surface concentration whereas the latter will decrease surface concentration. This relationship can be described by the dimensionless Péclet number, *Pe*. The Péclet number is the ratio of the evaporation rate, κ, and the diffusion coefficient, D, of a component i, as seen in Eq. 2. For a *Pe* close to 1 or smaller, the material will be able to diffuse quickly relative to receding droplet surface and thus will be evenly distributed. For a large *Pe*, the component is expected to be relatively immobile and therefore accumulate near the droplet surface.

$$Pe_i = \frac{\kappa}{8D_i} \quad (2)$$

Pe can be used to determine the surface enrichment of a given component. Surface enrichment is the surface concentration of a component, $c_{s,i}$, relative to its mean concentration within the droplet, $c_{m,i}$. Surface enrichment for a component with a *Pe* smaller than 20 can be approximated using Eq. 3 [38], in which the steady state surface enrichment value, E_{ss}, assumes that the solute concentration within the droplet changes at the same rate as the mean concentration.

$$E_{ss} = \frac{c_{s,i}}{c_{m,i}} \approx 1 + \frac{Pe_i}{5} + \frac{Pe_i^2}{100} - \frac{Pe_i^3}{4000} \quad (3)$$

Steady state surface enrichment for *Pe* values larger than 20 can be approximated using Eq. 4 [50]. Further discussion on *Pe* and surface enrichment can be found elsewhere [50].

$$E_{ss} \approx \frac{Pe_i}{3} + 0.363 \quad (4)$$

E_{ss} was used to approximate the time when a particle shell will form. The time at which shell formation is expected to start for components that do not crystallize is the time it takes a component to reach a concentration at the surface equivalent to its true density, $\tau_{t,i}$. The time at which shell formation is expected to start for components that do crystallize is the time that the component reaches critical supersaturation at the surface, $\tau_{s,i}$. The $\tau_{t,i}$ is given in Eq. 5, where $C_{0,i}$ is the initial concentration of component i and $\rho_{t,i}$ stands for its material true density, and τ_D is the droplet drying time. As the formulations investigated contain multiple components, true density of a mixture, $\rho_{t,mix}$, was calculated and substituted for $\rho_{t,i}$. The calculation of $\rho_{t,mix}$ is described elsewhere [37]. The $\tau_{s,i}$ is given in Eq. 6, where $C_{sol,i}$ is the solubility of component i.

$$\tau_{t,i} = \tau_D \left[1 - \left(\frac{C_{0,i}}{\rho_{t,i}} E_i \right)^{\frac{2}{3}} \right] \quad 5$$

$$\tau_{s,i} = \tau_D \left[1 - \left(\frac{C_{0,i}}{C_{sol,i}} E_i \right)^{\frac{2}{3}} \right] \quad 6$$

The evaporation rate of a pure water droplet at the drying gas temperature, 65 °C, is 3.7×10^{-9} m^2/s [51]. The diffusion coefficient of pullulan was approximated to be 2.8×10^{-11} m^2/s [37]. The diffusion coefficient for trehalose in water, D_{tre}. was calculated to be 3×10^{-10} m^2/s using Eq. 7 [52], where w_s is the mass fraction of solute and T is droplet temperature in K, i.e. 301 K [23]. This equation was obtained by fitting an equation to experimental data of trehalose diffusion in aqueous solutions [53].

$$D_{tre} = \frac{5\times10^{-8}}{e^{-13(w_s)^{1.1}}} e^{-1500\frac{e^{1.9\cdot w_s}}{T}} \quad 7$$

Diffusion coefficients for other solutes were approximated based on molecular size using the Einstein-Stokes equation. The GLA-SE nanoemulsion droplets were considered as a component for the sake of diffusion calculations. The diffusion coefficient of the nanoemulsion droplets has been previously approximated to be 5.3×10^{-12} m^2/s using the Einstein-Stokes equation, assuming that the nanoemulsion droplets remain stable as an aqueous dispersion and can be treated as nanoparticles [23].

The size of a peptide was approximated based on its mass using Eq. 8, assuming the peptide is in the shape of a sphere [54]. Eq. 8 determines R_{min} of a peptide, the minimum radius of a sphere that could contain its mass. R_{min} is given in nm and M is the molecular weight of the peptide, given in Da. Based on this equation, the diffusion coefficient for leucine was approximated to be 6.3×10^{-10} m^2/s and the diffusion coefficient for trileucine was approximated to be 4.5×10^{-10} m^2/s.

$$R_{min} = 0.066 M^{1/3} \quad 8$$

Distribution calculations for ID93 were not conducted as previous work has reported that an estimated 96% of the antigen is associated with the adjuvant [55]. The literature values for the density and solubility of the given components are summarized in Table 2. Table 2 also shows the calculated Pe and E_{ss} for each component.

Non-crystallizing components with a Pe near 1 and high solubility, such as trehalose, are expected to form solid particles later in the droplet lifetime with even component distribution. The Pe of both pullulan and the GLA-SE emulsion droplets was much greater than 1, suggesting that these components will accumulate near the surface of the drying

droplet. Previously, encapsulation of the vaccine candidate with trehalose via spray drying showed that the GLA-SE droplets are distributed throughout the trehalose matrix, with increasing radial concentration towards the particle surface [23].

A summary of the calculated particle formation parameters is given in Table 3, with calculations based on the values given in Table 2. These simplified calculations assume a constant *Pe* to provide an estimated timeline of the drying processes without looking into the detailed droplet drying steps. For example, formation of crystals will increase the *Pe* due to increasing component size, which will further facilitate surface enrichment. Similarly, increasing viscosity near the droplet surface due to increasing solute concentration over time will increase the *Pe* and thus facilitate shell formation. This particle formation model also neglects the effect of surface activity. Inclusion of these considerations results in very complex models that are outside the scope of this study.

Time to true density was calculated for trehalose and pullulan as neither are crystallizing systems under normal spray drying conditions. For trileucine, the phase separation is not fully understood at this time, however, previous studies have shown that it forms a shell soon after reaching saturation [1, 41, 40]. For this reason, the time to saturation was calculated for trileucine.

It is apparent that the trehalose will reach the true density of the given mixture relatively late (>90%) in the droplet lifetime for all formulations. The calculations predict that leucine reaches critical saturation relatively early (37.2%) in the droplet lifetime and therefore forms an outer shell composed of growing crystals. Pullulan was predicted to reach true density close to the same time as trehalose (93.0% and 87.9%), which suggests that the outer surface of these particles may be composed of both pullulan and trehalose. The model predicts that trileucine will accumulate on the surface and form a shell early in the drying process due to relatively short time to reach saturation (62.3% and 40.2%). Therefore, the model predicts that the chosen mass fractions are likely to result in partial to total particle surface coverage with the dispersibility enhancing agents for the chosen spray drying parameters.

2.4 Dry Powder Characterization

Field Emission Scanning Electron Microscopy (Zeiss Sigma FE-SEM; Carl Zeiss, Oberkochen, Germany) was used to determine particle morphology for the inhalable vaccine candidates. Powder samples were mounted either directly onto aluminum SEM stubs (Product 16111; Ted Pella, Inc.; Redding, CA, USA) or onto carbon tape placed over the stubs. The former method included scraping the powder against the stubs in order to intentionally crack particles open to view the interior structure. The latter method was implemented to avoid intentional destruction of the particles in order to view the exterior structure. These samples were placed in a desiccator connected to an in-house vacuum system for 1-4 days to remove the exposed nanoemulsion droplets and prevent damage to the electron microscope. Following desiccation, the samples were sputtered with a coating of 80% gold and 20% palladium (Leica ACE600 Carbon/Metal Coater; Concord, ON, Canada) to a thickness of 10-15 nm or with a coating of gold (Denton Vacuum Desk II Sputter Coater; Denton, Moorestown, NJ, USA) to a thickness of approximately 16 nm. Images

ranging from magnifications of 500 to 25000× were taken at a working distance of 5.4-6.8 mm using an accelerating voltage of 4-5 kV.

The solid phase of the powder was assessed by Raman spectroscopy to determine powder crystallinity for each spray-dried formulation using a custom dispersive Raman spectroscopy system. A detailed description of a similar apparatus has been published elsewhere [59]. All spectra were measured at a temperature of 22.0-23.0 °C and at less than 3% RH to prevent moisture exposure. Raman spectrum analysis was also conducted on crystalline trehalose, crystalline leucine, raw crystalline trileucine, crystalline Tris, and raw pullulan as references. Neat trehalose and neat trileucine from aqueous formulations were spray-dried with a bench top spray dryer under similar spray-drying conditions used in this study. These spray-dried trehalose and spray-dried trileucine powders were analyzed as amorphous references.

Reference spectra were also obtained for a liquid sample of squalene. The amorphous leucine spectrum was obtained by subtracting the water spectrum from a concentrated aqueous leucine solution (20 mg/mL) spectrum. It has been previously demonstrated that spectra of amorphous solids are similar to a concentrated aqueous solution of the solid [60].

Lung deposition was measured *in vitro* using a Next Generation Impactor (NGI) (Copley Scientific; Nottingham, UK) with an Alberta Idealized Throat (AIT) attachment. The AIT mimics the general geometry of a human mouth-throat [61]. Grgic et al. [62] established that particle deposition using the model is in agreement with human experimental extrathoracic deposition data. A simplified schematic of this set up is shown in Figure 1.

A commercial low resistance DPI (Seebri Breezhaler, Novartis International AG; Basel, Switzerland) was used to deliver the powder. The DPI has been characterized elsewhere [63]. The DPI was connected to the throat model using a custom 3D-printed mouthpiece adapter. A similar set up was used in Hoe et al. [45] and Carrigy et al. [37]. Inhalation flow rate was simulated via a critical flow controller (Critical Flow Controller Model TPK 2000, Copley Scientific Limited; Nottingham, UK) connected to a vacuum pump (Maxima M16C, Fisher Scientific; Ottawa, ON, Canada). This set up was utilized to obtain an assessment of loss due to extrathoracic powder deposition under normal use. A similar procedure was followed as given in Carrigy et al. [37]. Prior to the experiment, the impactor stages, the micro-orifice collector (MOC) and the interior of the throat model were coated with silicone spray (Molykote 316 Silicone Release Spray, Dow Corning Corporation; Midland, MI, USA) to mitigate particle bounce [64]. Powder was manually loaded into size 3 hydroxypropyl methylcellulose capsules (Quali-V-1; Qualicaps, Inc., Madrid, Spain) in a dry glovebox. Each capsule contained 41 ± 9 mg of powder. Actuation and inhalation was performed using three capsules in succession to obtain sufficient mass on the impactor stages and MOC for gravimetric analysis. Inhalation was simulated at an inspiratory flow rate of 100 L/min over 2.4 seconds to achieve 4 L of air withdrawal as per the USP 601 monograph [65]. Experiments were performed in triplicate and conducted under ambient conditions. A two-tailed student’s t-test was used for analysis, where statistically significant differences were reported for $p<0.05$.

All gravimetric measurements were conducted with a microbalance (ME204E, Mettler Toledo; Mississauga, ON, Canada). Capsules were weighed before and after powder loading to determine the mass of powder added. The DPI containing the loaded capsule was measured before and after actuation to determine the emitted dose, defined as the percentage of loaded mass that exited the inhaler. Lung dose was defined as the percentage of loaded mass that penetrated the throat model. Lung dose was calculated as the total powder deposition on the impactor stages relative to the loaded powder mass. Powder deposition was determined gravimetrically by measuring the stages before and after the experiment run. Correlation of mass distribution to particle size was based on stage cutoff diameters at 100 L/min flow rate, as determined elsewhere [66].

Mass median aerodynamic diameter, $d_{a,50}$, and geometric standard deviation, σ_g, of the deposited powder was calculated by fitting the data to a cumulative lognormal distribution function [37]. In this case, $d_{a,50}$ and σ_g measured are for the powder that has deposited within the impactor, not the size distribution of the spray-dried formulations themselves. Real-time sampling during production to obtain the $d_{a,50}$ and σ_g of the spray-dried formulations could not be completed due to equipment issues. Data fitting was done using the MATLAB (MathWorks Inc., Natick, MA, USA) “Curve Fitting” application. For a given stage, the cutoff diameter was plotted as the upper size limit for each bin, and the deposition fraction for each bin was calculated with respect to the total amount of powder deposited on the stages.

As previously indicated, inhalable aerosols can be administered through the intranasal or pulmonary route. The spray-dried powders investigated in this study were designed for delivery to the lungs through inhalation past the mouth. Powders designed for intranasal delivery through the nose would have to be assessed for deposition through other methods; however, this model can be used to provide an indication of powder dispersibility for a given formulation.

2.5 Reconstituted Powder Characterization

All samples were reconstituted to the feedstock concentrations with freshly dispensed MilliQ water for analysis. Nanoemulsion droplet diameter, polydispersity index, squalene concentration, GLA concentration, and ID93 presence were evaluated in the reconstituted powders. Similar experimental techniques were used previously to assess retention of vaccine components in spray-dried powder [23].

Mean hydrodynamic diameter and polydispersity of the nanoemulsion droplets in liquid formulations were measured using a dynamic light scattering technique (Zetasizer APS; Malvern, Worcestershire, UK). Polydispersity index was calculated as the standard deviation of the measured size distribution divided by the mean hydrodynamic diameter, squared. Details of the measurement process have been described elsewhere [67]. Reported average and standard deviation measurements for each sample are from the same sample analyzed 3 times.

Squalene content was quantified using a reverse phase HPLC method. Separation of squalene from sample was performed on an Agilent 1200 HPLC (1200 HPLC; Agilent

Technologies; Santa Clara, CA, USA) equipped with a silica-based, C18 reversed-phase column (Atlantis T3 Column; Waters; Elstree, UK). Column temperature was held constant at 30 °C and analyte detection was accomplished using a charged aerosol detector (Corona CAD; ESA Biosciences; Chelmsford, MA, USA). Mobile phase A contained 75:15:10 (v/v/v) methanol:chloroform:water, 1% (v/v) acetic acid, and 20 mM ammonium acetate and mobile phase B contained 50:50 (v/v) methanol:chloroform, 1% (v/v) acetic acid, and 20 mM ammonium acetate. Samples were diluted in mobile phase B and injected with a gradient over 30 minutes. Squalene content was quantitated by peak area. Concentration measurements were made by interpolation of a curve generated from standards fitted with a second order polynomial. Reported average and standard deviation measurements for each formulation are from two separately prepared HPLC samples.

GLA content was also quantified using a reverse phase HPLC method, in which separation of GLA from sample was done with the same equipment and the same mobile phases. Samples were diluted in mobile phase B and injected with a gradient over 18 minutes. Column temperature was held constant at 30 °C. GLA content was quantitated by peak height. Concentration measurements were made by interpolation of a curve generated from standards fitted with a second order polynomial. Reported average and standard deviation measurements for each formulation are from two separately prepared HPLC samples.

Due to insolubility in the HPLC buffers, samples that contained pullulan were diluted with the appropriate volume of mobile phase B, capped, and then centrifuged on an EZ-2 Mk2 centrifugal evaporator (Genevac LTD, Ipswich, England) for 20 minutes on the low boiling point setting with a maximum temperature set to 35°C. A 200 uL aliquot of sample was transferred to a new HPLC vial and then injected as normal. An internal standard containing either GLA or squalene was included to ensure no analyte loss upon centrifugation or transfer. Care was used not to disturb the pullulan pellet upon transfer.

The presence of ID93 in formulated samples was determined using SDS-PAGE. Gel samples were prepared by mixing 4X LDS Buffer (Thermo Fisher Scientific, Waltham, MA, USA) spiked with 5% (v/v) β-Mercaptoethanol, a 20% (w/v) sodium dodecyl sulfate solution (Thermo Fisher Scientific, Waltham MA, USA), and formulated sample in a 1:2:1 ratio. Prepared samples were heated in an 85°C water bath for 15 minutes, and then left to cool in a room temperature water bath. A precast, 4-20% Tris-Glycine SDS-PAGE gel (Thermo Fisher Scientific, Waltham, MA, USA) was prepared according to manufacturer's instructions for denaturing gel electrophoresis using Tris-Glycine SDS Running Buffer (Thermo Fisher Scientific, Waltham, MA, USA) and the recommended gel tank and power supply (Thermo Fisher Scientific, Waltham, MA, USA). Cooled gel samples were centrifuged at 2000 RPM in a benchtop centrifuge (Thermo Fisher Scientific, Waltham, MA, USA) for 2 minutes to collect the sample, and then briefly vortexed prior to loading onto the prepared gel. Mark12 ladder (data not shown) (Thermo Fisher Scientific, Waltham, MA, USA) was diluted 1:4 with freshly dispensed MilliQ water and also run on the gel as a molecular weight marker to confirm the expected migration of ID93 through the gel. The gel was run at 180V for 65 minutes, and then stained overnight using Sypro Ruby stain (Thermo Fisher Scientific, Waltham, MA, USA) according to the manufacturer's instructions. Stained gels were imaged using a gel imaging system (ChemiDoc; Bio-Rad, Mississauga, ON,

Canada) employing the manufacturer's settings for Sypro Ruby stain. Duplicate gels were run to confirm the presence or absence of the ID93 monomer band.

3 Results and Discussion

3.1 Particle Morphology

The particles for a given formulation exhibited consistent morphology. Representative SEM images of the inhalable vaccine candidates are shown in Figure 2. The spray-dried T formulation particles visually appear to be within respirable range. The particles' surface ranges from smooth to slightly dimpled, which was consistent with previous studies on spray drying ID93+GLA-SE vaccine with trehalose [23] and spray-dried bacteriophages encapsulated in trehalose [41, 68]. The smooth disaccharide particle surface is undesirable in terms of powder dispersibility as smooth surfaces are more cohesive than rugose surfaces. Interior analysis of cracked particles revealed the presence of many small voids. These voids are caused by the encapsulated nanoemulsion droplets within the amorphous trehalose matrix. Particle interiors feature either a large central void or many central voids (not shown) and exhibit a range of shell thicknesses, which was consistent with previous work [23].

Like the T formulation, the spray-dried T20Leu particles also appear to be within respirable range. Unlike the T formulation, T20Leu particle surfaces were rough, with many surface asperities. These surface asperities are likely individual leucine crystals. Similar surface morphology has been produced in spray-dried crystalline leucine and trehalose systems [34, 41]. The presence of leucine crystals at the particle surface was also predicted by the particle formation model; the formulation was designed such that leucine reached saturation on the surface early in the droplet evaporation process, providing the necessary time to form a shell on the surface before trehalose. Analysis of the cracked particle suggests that the T20Leu particles are composed of a trehalose core that transitioned into a crystalline leucine surface layer. Like the T particles, the nanoemulsion droplets are encapsulated within the spray-dried T20Leu particles.

Both the pullulan-containing formulations, T10Pul and T20Pul, produced dimpled particles which appear to be within respirable range. Increased number and depth of dimples was shown with increasing pullulan concentration. The surface particle morphology and increasing dimpling shown with increasing pullulan content were consistent with studies involving spray drying of trehalose-pullulan systems [37]. The dimpled morphology was not seen in the T particles, suggesting that the particle formation model correctly predicted that pullulan would enrich the surface. Interior particle morphology showed that the nanoemulsion droplets are encapsulated within the particle wall for both the pullulan containing formulations. Cracked particles appeared to be hollow, with a range of shell thicknesses (not shown). Unlike the T20Leu formulation, it was difficult to visually determine the presence or location of a radial pullulan-trehalose transition. Lack of clear transitional layer was expected as trehalose and pullulan are amorphous materials with no discernable visual difference at the given magnification.

The spray-dried formulations containing trileucine, T3Tri and T6Tri, produced highly folded particle surfaces, with increased wrinkles exhibited with increased trileucine concentration.

Exterior particle morphology was consistent with previous work on spray-dried trileucine-trehalose systems, which produced particles with low particle density, i.e. containing interior or exterior void space, or both [41, 40]. Increased corrugation of particles with increasing trileucine concentration had also been demonstrated in other systems [39]. The trileucine layer at the surface of the particles was predicted by the particle formation model as the time for trileucine saturation preceded time for trehalose precipitation. Folded surface morphology was due to the formation of a trileucine shell early in the particle formation process [40]. The particles collapsed due to the lack of early shell mechanical strength during the drying process and thus appear rugose. Increased trileucine concentration led to earlier shell formation; thus, the formulation with higher trileucine content showed particles with increased levels of folding. The T6Tri formulation's cracked particle image indicated that the nanoemulsion droplets were encapsulated within the particle. A cracked particle could not be found for the T3Tri formulation; however, the interior morphology was expected to be similar to T6Tri interior morphology due to formulation similarity.

3.2 Crystallinity Analysis

The Raman spectra of the inhalable vaccine candidates were analyzed to determine the solid phase of the spray-dried powder. The reference spectra for amorphous and crystalline trehalose, squalene, amorphous and crystalline leucine, pullulan, and amorphous and crystalline trileucine are shown in Figure 3. The ID93 and GLA contributions were not considered due to their low mass fraction. The Raman spectra for the inhalable vaccine candidates are shown in Figure 4. The residual spectrum after partial deconvolution is given under the respective formulation. Partial deconvolution was completed by subtracting the amorphous trehalose, squalene, and Tris reference spectra for all inhalable candidates. Additionally, for the formulations with dispersibility enhancing agents, crystalline leucine, pullulan, and amorphous trileucine reference spectra were subtracted from the T20Leu, T10Pul and T20Pul, and T3Tri and T6Tri formulations, respectively. Details on the deconvolution process are discussed elsewhere [60].

Deconvolution indicated that the trehalose component of all formulations was completely amorphous, as expected. The amorphous trehalose spectrum dominated the sample spectra as trehalose was the most abundant component in all formulations, with a designed mass fraction of 65-81%. All spray-dried vaccine powders, except for the T20Leu formulation, exhibit fully amorphous spectra, as indicated by the relatively low intensity residual spectra. The T20Leu spectrum features several crystalline leucine peaks, most noticeably at 966 and 984 cm^{-1}. The T20Leu formulation was designed to have a crystalline outer leucine layer, whereas all other formulations utilized dispersibility enhancing agents that were predicted to form an amorphous shell. These results provide additional evidence that the surface asperities shown in T20Leu morphology analysis are leucine crystals. Further spectral deconvolution indicated the presence of leucine in its amorphous state, which is consistent with the findings of other studies [34]. This study considered formulations with dispersibility enhancing agents ≤20% by mass fraction in order to maximize the adjuvant dose in the powder. However, Feng et al. [34] previously established that a critical crystallization time for the given system must be surpassed in order for the leucine component to be completely crystalline. Leucine crystallinity can be improved by increasing

the crystallization time, for example by either increasing the mass fraction or feed concentration.

3.3 Nanoemulsion Size Distribution

The vaccine nanoemulsion droplets' average diameter in the liquid formulation and reconstituted spray-dried powder are compared in Figure 5. The acceptable emulsion diameter range (80-160 nm) is represented by dashed red lines. The acceptance criteria are based on previously established quality control specifications for the nanoemulsion [69]. It is apparent that all formulations except T20Leu preserve emulsion diameter post-spray drying.

The trehalose control and both trileucine-containing formulations showed less than an 8% increase in emulsion diameter. These formulations had the highest relative mass fraction of trehalose, where trehalose composed 76-81% of the dry particles. High trehalose mass fraction increases the probability that the nanoemulsion droplets are surrounded by trehalose rather than other excipients. Similarly, a previous study involving spray-dried trehalose formulation at a higher feedstock concentration showed low increase in emulsion diameter of only 2-3% [23].

The T20Leu formulation's measured emulsion droplet diameter was the largest, increasing 145% to 225 nm. The significant increase in droplet diameter strongly suggests that leucine promotes instability of the GLA-SE membrane. The exhibited increase in emulsion diameter outside the acceptance limit removes the T20Leu candidate from consideration for further development. Crystallinity analysis results have shown that the leucine component in the T20Leu candidate is mostly crystalline. Studies on the lyophilization of the vaccine have shown that crystalline lyophilisate increased the GLA-SE particle size after reconstitution [22]. However, particle size analysis on a similar spray-dried formulation containing only 5% leucine mass fraction also showed an increase in emulsion droplet diameter from 94 nm to 178 nm on reconstitution (data not shown). It is highly likely that the leucine component of this spray-dried formulation with such a low leucine mass fraction (<10%) is primarily amorphous, according to Feng et al.'s work [34]. Therefore, crystallization of leucine may not be the only mechanism which destabilizes the GLA-SE membranes. It has been established that leucine molecules are able to penetrate DMPC monolayers in aqueous solutions [70]. Penetration of the lipid layer by an amino acid has been previously reported to cause membrane destabilization on dehydration and subsequent reconstitution [71]. Despite the similar molecular structure of leucine and trileucine, the trileucine-containing formulations did not exhibit a large increase in emulsion diameter.

Spray drying the pullulan-containing formulations led to an increase in emulsion droplet diameter of 28% and 53%, for T10Pul and T20Pul respectively. The increase in diameter for the T10Pul formulation is comparable to the increase in GLA-SE diameter of the lyophilized vaccine [22]. Increasing pullulan concentration appears to cause greater increase in nanoemulsion droplet diameter on reconstitution. The particle formation model predicted that pullulan enriches the surface, however, the time to true density occurs near the same time for the trehalose component. Particle morphology of these formulations suggests that the particles are likely composed of a pullulan and trehalose mixture, as there is no clear

distinction between the pullulan and trehalose layers. This distribution of components increases the likelihood of the emulsion droplets becoming encapsulated by pullulan, or a pullulan and trehalose mixture during drying. Addition of pullulan to stabilizing excipients has been previously shown to increase emulsion droplet size on reconstitution [72].

The polydispersity index of the nanoemulsion droplets in the liquid formulation and the reconstituted spray-dried powder for all inhalable vaccine candidates is shown in Figure 6. Maximum acceptable polydispersity index was limited to 0.2, as represented by the dashed red line. The results show that spray drying increased the polydispersity index of all inhalable vaccine candidates. This result is to be expected as some of the dispersed nanoemulsion droplets will inevitably collide and merge into larger ones during the spray drying process, causing the size distribution to deviate from perfect monodispersity. However, the measured polydispersity index of all formulations, except for the T20Leu candidate, was within the preset target criteria (<0.2). Increased polydispersity index further suggests that leucine destabilized the emulsion membrane.

3.4 Squalene and GLA Content

Comparison of squalene and GLA content between the feedstock and the reconstituted spray-dried powder for all inhalable candidates is shown in Table 4. Acceptance criteria was defined as ±20% of the target squalene concentration (5.73 mg/mL) and the target GLA concentration (3.33 μg/mL). No decrease in squalene content was detectable for any formulation, suggesting successful encapsulation of nanoemulsion droplets during spray drying. Therefore, addition of the chosen dispersibility enhancing agents did not negatively affect the encapsulation efficiency. Additionally, the successful retention of squalene indicates that the employed processing conditions were applicable for the different formulations. Reported higher values in squalene content after spray drying may be due to assay variability.

Similarly, it is apparent that no decrease in GLA content was detected for any formulation. The successful retention of GLA over spray drying suggests that the addition of the chosen dispersibility enhancing agents did not interfere with GLA stabilization via trehalose. Reported higher values in GLA content after spray drying may be due to assay variability.

3.5 ID93 Retention

ID93 presence was measured using SDS-PAGE analysis. Stained gels of the inhalable vaccine candidates and a control are shown in Figure 7. The ID93 band was present in all formulations with the exception of those that contained pullulan.

The absence of an ID93 band in the T10Pul and T20Pul formulations suggests that the addition of pullulan negatively affects the formulations' ability to stabilize the ID93 protein, thus eliminating these formulations from consideration as inhalable candidates. Results were repeated for the pullulan-containing formulations (not shown) to confirm the absence of the ID93 band. Pullulan and trehalose excipient mixtures have successfully stabilized air-dried HSV-2 vaccine, however, pullulan alone has been shown to offer poor protection against desiccation, with significant loss in titer on drying and complete loss after only a week of

storage at room temperature [36]. Further investigation is required to determine why the ID93 band was not present in the pullulan-containing formulations.

3.6 Aerosol Performance

Successful respiratory pharmaceutical delivery requires that an appropriate dose be delivered to the lung and that the powder deposits in the appropriate region of the lung. In this study, a throat model connected to an impactor was utilized to assess the dosage lost to mouth-throat deposition for each candidate under normal use. Lung dose was reported in this study rather than the commonly used measurement of fine particle fraction, the fraction of deposited particles with a $d_a \leq 5$ μm. Fine particle fraction was not reported in this study as the set up utilized allows for the lung dose to be reported directly for a given candidate.

Table 5 compares the inhalable vaccine candidates' overall aerosol performance and size distribution of the lung dose, that is, the powder which penetrated the throat model and deposited within the impactor. Mass distribution of each candidate, shown in Figure 8, was used to calculate size distribution. The bracketed $d_{a,50}$ values are greater than the minimum particle size expected to deposit on Stage 1 (6.12 μm). The larger value indicates that these powders experienced greater deposition in the throat and on the first stage of the impactor due to significant particle aggregation.

Emitted dose for all inhalable candidates ranged from 84-97%. These results are very high for an experimental dry powder formulation, even outperforming some commercial DPI products [73]. However, the candidates exhibited markedly different performances in terms of lung dose.

The T formulation had the lowest mean lung dose of the investigated candidates. These results are expected as the T formulation did not include any dispersibility enhancing agents. The $d_{a,50}$ of the T formulation was low compared to the other formulations, which would typically suggest that the formulation was well-dispersed. However, as shown in Figure 8, the T formulation deposited the lowest powder mass on Stage 1 as most of the powder aggregates deposited in the throat model instead. The lack of powder deposited on the later stages of the impactor further indicates that the T formulation was not well-dispersed. The low measured $d_{a,50}$ is due to the much higher level of particle aggregation as compared to the others. The high level of aggregation led to most of the larger aggregates depositing in the throat prior to the impactor stages, as evidenced by the lowest lung dose.

The T20Leu formulation almost doubled lung dose as compared to the T formulation. This increase in aerosol performance was due to the designed rugose crystalline leucine surface layer of the T20Leu formulation, the presence of which was confirmed by morphology and solid state analysis. As discussed previously, increased rugosity and stiffness of the surface decreases the force of cohesion between particles and therefore make the powder more dispersible. These results showing that a crystalline leucine surface layer increases dispersibility of the powder was consistent with other studies. However, the fact that the measured $d_{a,50}$ was higher than the theoretical values suggests that many particles remained aggregated after exiting the DPI. Feng et al. [34] demonstrated that increasing leucine concentration in spray-dried leucine-trehalose systems improves dispersibility of the powder.

Similarly, Arora et al. [74] demonstrated that spray drying the drug voriconazole with 20% leucine increased dispersibility when tested using a similar DPI and NGI set up. Emitted dose for the spray-dried voriconazole formulation without leucine was only 58% but increased to 82% for the formulation containing 20% leucine. However, the dispersibility of a crystalline formulation is not solely dependent on the presence of surface crystals but also on their size and the number density of these surface crystals. Raula et al. [75] coated salbutamol sulphate microparticles with leucine at different saturation levels and assessed dispersibility of the powders using a commercial DPI with a custom inhalation simulator. Morphological analysis found that increasing leucine content led to an increase in size and number density of asperities on the surface of the particles. The leucine coating improved particle dispersity over the uncoated particles, however, the authors found that the emitted dose decreased with further increasing leucine content. Smaller surface asperities may be more beneficial for improving particle dispersity as larger surface asperities may not reduce contact area and instead introduce mechanical interlocking forces between particles.

Neither of the pullulan-containing formulations improved lung dose significantly as compared to the T formulation. Particle surface morphology analysis showed that the addition of pullulan produced dented particles that still maintained an overall smooth surface. The dented surface morphology did not sufficiently reduce the forces of cohesion between the particles. The particle surface dimples may have been detrimental in the present study due to the polydispersity of the powder as it is possible that the dimples in the larger particles may have provided an area for smaller particles to settle into, increasing the contact area between the two. Similarly, the measured particle sizes, which were larger than the theoretical predictions, also suggest a high level of particle aggregation. Particle dimples are shown to a higher extent with increased pullulan concentration, possibly explaining the lower aerosol performance of the T20Pul formulation compared to TIOPul. Previously, Carrigy et al. [41] showed that spray-dried pullulan-trehalose systems at different concentrations either improved or had the same aerosol performance as spray-dried trehalose microparticles. Their results found that a formulation containing 10% pullulan and 90% trehalose by mass improved the aerosol performance compared to spray-dried trehalose alone, however, a 40% pullulan and 60% trehalose formulation had an aerosol performance similar to that of trehalose alone. This suggests a point of diminishing returns for the addition of pullulan to improve powder dispersibility.

It is apparent that the trileucine-containing formulations, T3Tri and T6Tri, performed the best out of the tested inhalable vaccine candidates. These formulations were the only ones found to significantly improve the mean lung dose as compared to the T formulation. The measured 33-34% lung dose of these formulations is comparable to the lung dose obtained with commercial products. Ruzycki et al. [76] found that the lung dose, as a percentage of label claim, of six commercial DPI's ranged from 19-35% at the minimum efficacious flow rate and 22-53% at a standard pressure drop. Similarly, the Borgstrom et al. [77] found that lung dose of two commercial Turbuhaler DPIs in asthmatic patients averaged 20.8% and 16.9%. The measured $d_{a,50}$ for the trileucine-containing formulations was also the lowest out of all inhalable candidates. The average σ_g values of the trileucine-containing formulations were the largest, indicating a wide range in particle size of the deposited powder. The dispersed powder size range is illustrated in Figure 8 where the trileucine containing

formulations were the only candidates to exhibit powder deposition on all NGI stages and the MOC. Altogether, these results indicate that the inclusion of trileucine led to superior ability to disperse the smaller particles in the powder.

The addition of trileucine produced the greatest change in particle morphology, where analysis indicated the production of large particles that were outside the intended size range. However, the SEM images showed that these particles are thin-shelled and hollow; this morphology suggests that the particles have low density and therefore, the aerodynamic diameter of the particles is much smaller than the geometric diameter. Powders composed of geometrically large particles are easier to disperse as the aerodynamic forces, which act to disperse the powder during inhalation, increase with increasing particle diameter [27]. Additionally, the designed wrinkled surface morphology due to trileucine surface accumulation decreases contact area between particles, theoretically improving powder dispersibility. Accumulation of trileucine on the particle surface is also expected to reduce surface energy. Previously, increased trileucine content has been shown to improve powder dispersibility through reduction of particle surface energy even when particle morphology was no longer changing with increasing concentration [39]. These factors likely all contributed to the improved aerosol performance of the trileucine-containing formulations in this study. Based on the high dispersibility potential, the trileucine-containing formulations are the only ones which can deliver a portion of the vaccine in the peripheral region of the lung. Differences in the aerosol performance of the T3Tri and the T6Tri formulations were statistically insignificant, suggesting a similar level of trileucine particle surface coverage for both the T3Tri and the T6Tri formulations.

None of the inhalable vaccine candidates was completely dispersed to the predicted primary aerodynamic particle size of 3-4 μm. However, aerosol performance assessment was completed with an unoptimized DPI in this study. As explicitly noted in de Boer et al.'s [73] review paper on dry powder inhalation, successful pulmonary delivery of vaccines often requires further DPI development to improve efficiency and deep lung delivery. Recently, Sibum et al. assessed the aerosol performance and stability of isoniazid spray-dried with leucine or trileucine [78]. Their results found that use of the Cyclops DPI over a Twincer DPI improved the emitted dose of the 3% leucine, 5% leucine, and 3% trileucine formulations by approximately 40%, 25%, and 10%, respectively.

4 Conclusion

This study demonstrates the use of particle engineering principles in the investigation of various excipients to improve aerosol performance of a complex inhalable vaccine formulation. In this study an excipient system was developed that encapsulated an adjuvanted subunit TB vaccine candidate formulated as a nanoemulsion via spray drying. Results found that the adjuvant system was successfully stabilized, with evidence shown that the antigen is present in the spray dried powder. Promising aerosol performance was achieved by adding a dispersibility enhancer, trileucine, to the formulation. This study also demonstrated the potential of the vaccine to be delivered as a respirable dosage to human lungs via inhalation using a DPI. Published work on spray drying vaccines formulated as lipid-based dispersions has primarily focused on stabilization.

The demonstrated potential for pulmonary vaccine delivery creates options for vaccines, such as the model TB vaccine investigated in this study, to be administered via an alternative route to traditional parenteral injection. Intranasal delivery of the spray-dried vaccine may be possible with adjustments to some particle properties, such as the size of the spray-dried particles, or switching to another delivery device. Administration through inhalation mitigates risks associated with needle delivery such as needlestick injuries, needlestick waste, and transfer of bloodborne illnesses. Nevertheless, more work is needed to further characterize the storage stability of the inhalable spray-dried vaccine. Additionally, while the potential for pulmonary delivery has been demonstrated at this point it is not known which administration route will elicit the strongest immune response for this particular TB vaccine candidate. Preclinical *in vivo* studies must be completed to compare the effects of vaccine administration via different routes on immunogenicity and efficacy.

Acknowledgements and Disclosures

This work was supported by federal funds from the National Institute of Allergy and Infectious Diseases, National Institutes of Health, Department of Health and Human Services, under Contract HHSN272201400041C. The authors would also like to thank Conor Ruzycki for designing the custom mouthpiece adaptor.

References

[1]. Carrigy NB and Vehring R, “Engineering stable spray-dried biologic powder for inhalation,” in Pharmacuetical Inhalation Aerosol Technology, Hickey AJ and da Rocha S, Eds., Boca Raton, CRC Press, 2019, pp. 291–326.

[2]. LeClair DA, Li L, Rahman N, Cranston ED, Xing Z and Thompson MR, “Stabilization of HSV-2 viral candidate by spray drying,” International Journal of Pharmaceutics, vol. 569, pp. 1–10, 2019.

[3]. Kanojia G, Willems G-J, Frijlink HW, Kersten GFA, Soema PC and Amorij J-P, “A design of experiment approach to predict product and process parameters for a spray dried influenza vaccine,” Inernational Journal of Pharmaceutics, vol. 511, pp. 198–1111, 2016.

[4]. Jones RM, Burke M, Dubose D, Chichester JA, Manceva S, Horsey A, Streatfield SJ, Breit J and Yusibov V, “Stability and pre-formulation development of a plant-produced anthrax vaccine candidate,” Vaccine, vol. 35, pp. 5463–5470, 2017. [PubMed: 28117174]

[5]. Toniolo SP, Afkhami S, Mahmood A, Fradin C, Lichty BD, Miller MS, Xing Z, Cranston ED and Thompson MR, “Excipient selection for thermally stable enveloped and non-enveloped viral vaccine platforms in dry powders,” International Journal of Pharmaceutics, vol. 561, pp. 66–73, 2019. [PubMed: 30825554]

[6]. Price DN, Kunda NK, Ellis R and Muttil P, “Design and optimization of a temperature-stable dry powder BCG vaccine,” Pharmaceutical Research, vol. 37, no. 11, pp. 1–14, 2020.

[7]. Sou T, Morton DAV, Williamson M, Meeusen EN, Kaminskas LM and McIntosh MP, “Spray-dried influenza antigen with trehalose and leucine produces an aerosolizable powder vaccine formulation that induces strong systemic and mucosal immunity after pulmonary administration,” Journal of Aerosol Medicine and Pulmonary Drug Delivery, vol. 28, no. 5, pp. 361–371, 2015. [PubMed: 25714115]

[8]. Kunda NK, Alfagih IM, Miyaji EN, Figueiredo DB, Goncalves VM, Ferreira DM, Dennison SR, Somavarapu S, Hutcheon GA and Saleem IY, “Pulmonary dry powder vaccine of pneumococcal antigen loaded nanoparticles,” International Journal of Pharmaceutics, vol. 495, no. 2, pp. 903–912, 2015. [PubMed: 26387622]

[9]. Argarkhedkar S, Kulkarni PS, Winston S, Sievers R, Dhere RM, Gunale B, Powell K, Rota PA, Papania M and M. a. group, “Safety and immunogenicity of dry powder measles vaccine administered by inhalation: A randomized controlled Phase 1 clinical trial,” Vaccine, vol. 32, pp. 6791–6797, 2014. [PubMed: 25446830]

[10]. Aguilo N, Alvarez-Arguedas S, Uranga S, Marinova D, Monzon M, Badiola J and Martin C, "Pulmonary but not subcutaneous delivery of BCG vaccine confers protection to tuberculosis-susceptible mice by an interleukin 17-dependent mechanism," Journal of Infectious Diseases, vol. 213, no.5,pp.813–839, 2016.

[11]. World Health Organization, "Global tuberculosis report," World Health Organization, Geneva, 2019.

[12]. Flynn JL, Chan J and Llin PL, "Macrophages and control of granulomatous inflammation in tuberculosis," Mucosal Immunology, vol. 4, no. 3, pp. 271–278, 2011. [PubMed: 21430653]

[13]. Chen L, Wang J, Zganiacz A and Xing Z, "Single intranasal mucosal Mycobacterium bovis BCG vaccination confers improved protection compared to subcutaneous vaccination against pulmonary tuberculosis," Infection and Immunity, vol. 72, no. 1, pp. 238–246, 2004. [PubMed: 14688101]

[14]. Derrick SC, Kolibab K, Yang A and Morris SL, "Intranasal administration of Mycobacterium bovis BCG induces superior protection against aerosol infection with Mycobacterium tuberculosis in mice," Clinical and Vaccine Immunology, vol. 21, no. 10, pp. 1443–1451, 2014. [PubMed: 25143340]

[15]. Verreck FAW, Tchilian EZ, Vervenne RA, Sombroek CC, Kondova I, Eissen OA, Sommandas V, van der Werff NM, Verschoor E, Braskamp G, Bakker J, Langermans JAM, Beverley PCL and Kocken CHM, "Variable BCG efficacy in rhesus populations: pulmonary BCG provides protection where standard intradermal vaccination fails," Tuberculosis, vol. 104, pp. 46–57, 2017. [PubMed: 28454649]

[16]. Andersen P and Doherty TM, "The success and failure of BCG - implications for a novel tuberculosis vaccine," Nature Reviews Microbiology, vol. 3, pp. 656–662, 2005. [PubMed: 16012514]

[17]. Hesseling AC, Johnson LF, Jaspan H, Cotton MF, Whitelaw A, Schaaf HS, Fine PEM, Eley BS, Marais BJ, Nuttall J, Beyers N and Godfrey-Faussett G, "Disseminated bacille Calmette-Guerin disease in HIV-infected South African infants," Bulletin of the World Health Organization, vol. 87, pp. 505–511, 2009. [PubMed: 19649364]

[18]. Bertholet S, Ireton GC, Ordway DJ, Plessner Windish H, Pine SO, Kahn M, Phan T, Orme IM, Vedvick TS, Baldwin SL, Coler RN and Reed SG, "A defined tuberculosis vaccine candidate boosts BCG and protects against multidrug-resistant Mycobaterium tuberculosis," Science Translational Medicine, vol. 2, no. 53, pp. 53–74, 2010.

[19]. World Health Organization (WHO), "Temperature sensitivity of vaccines," 8 2006 [Online]. Available: https://apps.who.int/iris/handle/10665/69387. [Accessed 17 April 2020].

[20]. World Health Organization, "WHO Preferred Product Characteristics for New Tuberculosis Vaccines," World Health Organization, Geneva, 2018.

[21]. Orr MT, Kramer RM, Barnes LV, Dowling QM, Desbien AL, Beebe EA, Laurance JD, Fox CB, Reed SG, Coler RN and Vedvick TS, "Elimination of the cold-chain dependance of a nanoemulsion adjuvant vaccine against tuberculois by lyophilization," Journal of Controlled Release, vol. 10, no. 177, pp. 20–26, 2014.

[22]. Kramer RM, Archer MC, Dubois N, Dubois Cauwelaert N, Beebe EA, Huang P.-w. D., Dowling QM, Schwartz AM, Fedor DM, Vedvick TS and Fox CB, "Development of a thermostable nanoemulsion adjuvanted vaccine against tuberculosis using a design-of-experiments approach," International Journal of Nanomedicine, vol. 13, pp. 3689–3711, 2018. [PubMed: 29983563]

[23]. Gomez M, Archer M, Barona D, Wang H, Ordoubadi M, Bin Karim S, Carrigy NB, Wang Z, McCollum J, Press C, Gerhardt A, Fox CB, Kramer RM and Vehring R, "Microparticle Encapsulation of Subunit Tuberculosis Vaccine Candidate containing Nanoemulsion Adjuvants via Spray Drying," Manuscript submitted for publication, 2020.

[24]. Infectious Disease Research Institute, "Identifier: NCT03722472, Phase 1 Clinical Trial of Single-Vial ID93 + GLA-SE in Healthy Adults," 3 9 2019 [Online]. Available: https://clinicaltrials.gov/ct2/show/NCT03722472?term=id93&draw=2&rank=1. [Accessed 23 April 2020].

[25]. Langford A, Bhatnagar B, Walters R, Tchessalov S and Ohtake S, "Drying technologies for biopharmaceutical applications: Recent developments and future direction," Drying Technology, vol. 36, no. 6, pp. 677–687, 2018.

[26]. McAdams D, Chen D and Kristensen D, “Spray drying and vaccine stabilization,” Expert Review of Vaccines, vol. 11, no. 10, pp. 1211–1219, 2012. [PubMed: 23176654]

[27]. Finlay WH, The Mechanics of Inhaled Pharmaceutical Aerosols: An Introduction, 2nd ed., Academic Press, 2019.

[28]. Kanojia G, ten Have R, Soema PC, Frijlink H, Amorij P and Kersten G, “Developments in forumulation and delivery of spray dried vaccines,” Human Vaccines & Immunotherapeutics, vol. 13, no. 10, pp. 2364–2378, 2017. [PubMed: 28925794]

[29]. Bahamondez-Canas TF and Cui Z, “Intranasal immunization with dry powder vaccines,” European Journal of Pharmaceutics and Biopharmaceutics, vol. 122, pp. 167–175, 2018. [PubMed: 29122735]

[30]. Hickey AJ, Durham PG, Dharmadhikari A and Nardell EA, “Inhaled drug treatment for tuberculosis: Past progress and future prospects,” Journal of Controlled Release, vol. 240, pp. 127–134, 2016. [PubMed: 26596254]

[31]. Shang Y, Dong J, Inthavong K and Tu J, “Comparative numerical modeling of inhaled micronsized particle deposition in human and rate nasal cavities,” Inhalation Toxicology, vol. 27, no. 13, pp. 694–705, 2015. [PubMed: 26406158]

[32]. Usmani OS, Biddiscombe MS and Barnes PJ, “Regional lung deposition and bronchodilator response as a function of beta2-agonist particle size,” American Journal of Respiratory and Critical Care Medicine, vol. 172, no. 12, pp. 1497–1504, 2005. [PubMed: 16192448]

[33]. Leung SSY, Parmasivam T, Nguyen A, Gengenbach T, Carter EA, Carrigy NB, Wang H, Vehring R, Finlay WH, Morales S, Britton WJ, Kutter E and Chan H-K, “Effect of storage temperature on the stability of spray dried bacteriophage powders,” European Journal of Pharmaceutics and Biopharmaceutics, vol. 127, pp. 213–222, 2018. [PubMed: 29486303]

[34]. Feng AL, Boraey MA, Gwin MA, Finlay PR, Kuehl PJ and Vehring R, “Mechanistic models facilitate efficient development of leucine containing microparticles for pulmonary drug delivery,” International Journal of Pharmaceutics, vol. 409, pp. 156–163, 2011. [PubMed: 21356284]

[35]. Li L, Sun S, Parumasivam T, Denman JA, Gengenbach T, Tang P, Mao S and Chan H-K, “L-Leucine as an excipient against moisture on in vitro aerosolization performances of highly hygroscopic spray-dried powders,” European Journal of Pharmaceutics and Biopharmaceutics, vol. 102, pp.132–141, 2016. [PubMed: 26970252]

[36]. Leung V, Mapletoft J, Zhang A, Lee A, Vahedi F, Chew M, Szewczyk A, Jahanshahi-Anhubhi S, Ang J, Cowbrough B, Miller MS, Ashkar A and Filipe CDM, “Thermal stabilization of viral vaccines in low-cost sugar films,” Scientific Reports, vol. 9, no. 7631, 2019.

[37]. Carrigy NB, Ordoubadi M, Liu Y, Melhem O, Barona D, Wang H, Milburn L, Ruzycki CA, Finlay WH and Vehring R, “Amorphous pullulan trehalose microparticle platform for respiratory delivery,” International Journal of Pharmaceutics, vol. 563, pp. 156–168, 2019. [PubMed: 30951858]

[38]. Vehring R, “Pharmaceutical Particle Engineering via Spray Drying,” Pharmaceutical Research, vol. 25, no. 5, pp.999–1022, 2008. [PubMed: 18040761]

[39]. Lechuga-Ballesteros D, Charan C, Stults CL, Stevenson CL, Miller DP, Vehring R, Tep V and Kuo M-C, “Trileucine Improves Aerosol Performance and Stability of Spray-Dried Powders for Inhalation,” Journal of Pharmaceutical Sciences, vol. 97, no. 1, pp. 287–302, 2008. [PubMed: 17823950]

[40]. Wang H, Nobes DS and Vehring R, “Particle Surface Roughness Improves Colloidal Stability of Pressured Pharmaceutical Suspensions,” Pharmaceutical Research, vol. 36, no. 43, 2019.

[41]. Carrigy NB, Liang L, Wang H, Kariuki S, Nagel TE, Connerton IF and Vehring R, “Trileucine and pullulan improve anti-Campylobacter bacteriophage stability in engineered spray-dried microparticles,” Annals of Biomedical Engineering, vol. 48, pp. 1169–1180, 2019. [PubMed: 31845128]

[42]. Ivey J, Bhambri P, Lewis D, Church T, Finlay W and Vehring R, “Dried corticosteroid particle formation from evaporating monodisperse propellant solution droplets,” in AAPS Annual Meeting and Exposition, Denver, 2016.

[43]. Grasmeijer N, Tiraboschi V, Woerdenbag HJ, Frijlink HW and Hinrichs WLJ, “Identifying critical process steps to protein stability during spray drying using a vibrating mesh or a two-fluid nozzle,” European Journal of Pharmaceutical Sciences, vol. 128, pp. 152–157, 2019. [PubMed: 30521944]

[44]. Carrigy NB, Liang L, Wang H, Kariuki S, Nagel TE, Connerton IF and Vehring R, “Spray-dried anti-Campylobacter bacteriophage CP30A powder suitable for global distribution without cold chain infrastructure,” International Journal of Pharmaceutics, vol. 569, pp. 1–9, 2019.

[45]. Hoe S, Ivey JW, Boraey MA, Shamsaddini-Shahrbabak A, Javaheri E, Sadaf M, Finlay WH and Vehring R, “Use of a fundamental approach to spray-drying formulation design to facilitate the development of multi-component dry powder aerosols for respiratory drug delivery,” Pharmaceutical Research, vol. 32, no. 2, pp. 449–465, February 2014.

[46]. Ivey JW and Vehring R, “The use of modeling in spray drying of emulsions and suspensions accelerates formulation and process development,” Computers and Chemical Engineering, vol. 34, pp.1036–1040, 2010.

[47]. Jones JR, Prime D, Leaper MC, Richardson DJ, Rielly CD and Stapley AGF, “Effect of processing variables and bulk composition on the surface composition of spray dried powders of a model food system,” Journal of Food Engineering, vol. 118, pp. 19–30, 2013.

[48]. Wang Y, Liu W, Chen XD and Selomulya C, “Micro-encapsulation and stabilization of DHA containing fishoil in protein-based emulsion through mono-disperse droplet spray dryer,” Journal of Food Engineering, vol. 175, pp. 74–84, 2016.

[49]. Li Q , Rudolph V and Peukert W, “London-van der Waals adhesiveness of rough particles,” Powder Technology, vol. 161, pp. 248–255, 2006.

[50]. Boraey MA and Vehring R, “Diffusion controlled formation of microparticles,” Journal of Aerosol Science, vol. 67, pp. 131–143, 2014.

[51]. Vehring R, Foss WR and Lechuga-Ballesteros D, “Particle formation in spray drying,” Aerosol Science, vol. 38, pp. 728–746, 2007.

[52]. Grasmeijer N, Frijlink HW and Hinrichs WLJ, “Model to predict inhomogeneous protein-sugar distribution in powders prepared by spray drying,” Journal of Aerosol Science, vol. 101, pp. 22–33, 2016.

[53]. Ekdawi-Sever N and de Pablo JJ, “Diffusion of sucross and a,a-trehalose in aqueous solutions,” Journal of Physical Chemistry A, vol. 107, pp. 936–943, 2003.

[54]. Erickson HP, “Size and shape of protein molecules at the nanometer level determined by sedimentation, gel filtration, and electron microscopy,” Biological Procedures Online, vol. 11, pp. 32–51, 2009. [PubMed: 19495910]

[55]. Orr MT, Fox CB, Baldwin SL, Sivananthan SJ, Lucas E, Lin S, Phan T, Moon JJ, Vedvick TS, Reed SG and Coler RN, “Adjuvant formulation structure and composition are critical for the development of an effective vaccine against tuberculosis,” Journal of Controlled Release, vol. 172, pp. 190–200, 2013. [PubMed: 23933525]

[56]. Sigma-Aldrich, “Safety Data Sheet: L-Leucine,” 15 1 2020 [Online]. Available: https://www.sigmaaldrich.com/catalog/product/sigma/l8000?lang=en&region=US. [Accessed 5 April 2020].

[57]. Sangon Biotech, “Safety Data Sheets: Pullulan,” 6 2 2018 [Online]. Available: https://www.sangon.com/productImage/SDS/A506209/A506209_EN_S.pdf. [Accessed 5 April 2020].

[58]. Leathers TD, “Biotechnical production and applications of pullulan,” Applied Microbiology and Biotechnology, vol. 62, pp. 468–473, 2003. [PubMed: 12830329]

[59]. Wang H, Barona D, Oladepo S, Williams L, Hoe S, Lechuga-Ballesteros D and Vehring R, “Macro-Raman spectroscopy for bulk composition and homogeneity analysis of multi-component pharmaceutical powders,” Journal of Pharmaceutical and Biomedical Analysis, vol. 141, pp. 180–191, 2017. [PubMed: 28448887]

[60]. Vehring R, “Red-excitation dispersive Raman spectroscopy is a suitable technique for solid-state analysis of respirable pharmaceutical powders,” Applied Spectroscopy , vol. 59, no. 3, pp. 286–292, 2005. [PubMed: 15901308]

[61]. Zhang Y, Gilbertson K and Finlay WH, “In vivo-in vitro comparison of deposition in three mouth-throat models with Qvar and Turbuhaler inhalers,” Journal of Aerosol Medicine, vol. 20, pp. 227–235, 2007. [PubMed: 17894531]

[62]. Grgic B, Finlay WH and Heenan A, “Regional aerosol deposition and flow measurements in an idealized mouth and throat,” Journal of Aerosol Science, vol. 35, pp. 21–32, 2004.

[63]. Pavkov R, Mueller S, Fiebich K, Singh D, Stowasser F, Pignatelli G, Walter B, Ziegler D, Dalvi M, Dederichs J and Rietveld I, “Characteristics of a capsule based dry powder inhaler for the delivery of indacterol,” Current Medial Research and Opinion, vol. 26, no. 11, pp. 2527–2533, 2010.

[64]. Zhou Y, Sun J and Cheng Y-S, “Comparison of deposition in the USP and physical mouth-throat models with solid and liquid particles,” Journal of Aerosol Medicine and Pulmonary Drug Delivery, vol. 24, no. 6, pp. 277–284, 2011. [PubMed: 21732711]

[65]. United States Pharmacopeia, “<601> Aerosols, nasal sprays, metered-dose inhalers, and dry powder inhalers,” 2017.

[66]. Marple VA, Roberts DL, Romay FJ, Miller NC, Truman KG, Van Oort M, Olsson B, Holroyd MJ, Mitchell JP and Hochrainer D, “Next Generation Pharmaceutical Impactor (A New Impactor for Pharmaceutical Inhaler Testing) Part 1: Design,” Journal of Aerosol Medicine, vol. 16, no. 3, pp.283–299, 2003. [PubMed: 14572326]

[67]. Chan MY, Dowling QM, Sivananthan SJ and Kramer RM, “Particle sizing of nanoparticle adjuvant formulations by dynamic light scattering (DLS) and nanoparticle tracking analysis (NTA),” Methods in Molecular Biology, vol. 1494, pp. 239–252, 2017. [PubMed: 27718198]

[68]. Vandenheuvel D, Meesus J, Lavigne R and Van den Mooter G, “Instability of bacteriophages in spray-dried trehalose powders is caused by crystallization of the matrix,” International Journal of Pharmaceutics, vol. 472, pp. 202–205, 2014. [PubMed: 24950368]

[69]. Fox CB, Huynh C, O’Hara MK and Onu A, “Technology transfer of oil-in-water emulsion adjuvant manufacturing for pandemic influenza vaccine production in Romania,” Vaccine, vol. 31, pp.1633–1640, 2013. [PubMed: 23103197]

[70]. Nakagaki M and Okamura E, “Penetration leucine and norleucine into lecithin monolayers from underlying aqueous solutions,” Bulletin of the Chemical Society of Japan, vol. 55, no. 11, pp. 3381–3385, 1982.

[71]. Chen L, Gan L, Liu M, Fan R, Xu Z, Zhixian H and Chen L, “Destabilization of artificial biomembrane induced by the penetration of tryptophan,” Applied Surface Science, vol. 257, pp. 5070–5076, 2011.

[72]. Bakry AM, Fang Z, Ni Y, Cheng H, Chen YQ and Liang L, “Stability of tuna oil and tuna oil/peppermint oil blend microencapsulated using whey protein isolate in combination with carboxymethyl cellulose or pullulan,” Food Hydrocolloids, vol. 60, pp. 559–571, 2016.

[73]. de Boer AH, Hagedoorn P, Hoppentocht M, Buttini F, Grasmeijer F and Frijlink HW, “Dry powder inhalation: past, present and future,” Expert Opinion on Drug Delivery, vol. 14, no. 4, pp. 499–512, 2017. [PubMed: 27534768]

[74]. Arora S, Haghi M, Young PM, Kappl M, Traini D and Jian S, “Highly respirable dry powder inhalable formulation of voriconazole with enhanced pulmonary bioavailability,” Expert Opinion on Drug Delivery, vol. 13, no. 2, pp. 183–193, 2016. [PubMed: 26609733]

[75]. Raula J, Thielmann F, Naderi M, Lehto V-P and Kauppinen EI, “Investigations on particle surface characteristics vs. dispersion behaviour of L-leucine coated carrier-free inhalable powders,” International Journal of Pharmaceutics, vol. 385, pp. 79–85, 2010. [PubMed: 19879344]

[76]. Ruzycki CA, Martin AR, Vehring R and Finlay WH, “An In Vitro Examination of the Effects of Altitude on Dry Powder Inhaler Performance,” Journal of Aerosol Medicine and Pulmonary Drug Delivery, vol. 31, pp. 221–236, 2018. [PubMed: 29125912]

[77]. Borgstrom L, Bengtsson T, Derom E and Pauwels R, “Variability in lung deposition of inhaled drug, within and between asthmatic patients, with a pMDI and a dry powder inhaler, Turbuhaler,” International Journal of Pharmaceutics, vol. 193, pp. 227–230, 2000. [PubMed: 10606786]

[78]. Sibum I, Hagedoorn P, Kluitman MPG, Kloezen M, Frijlink HW and Grasmeijer F, “Dispersity and storage stability optimization of high dose ioniazid dry powder inhalation formulations with L-leucine or trileucine,” Pharmaceutics, vol. 12, no. 24, pp. 1–14, 2020.

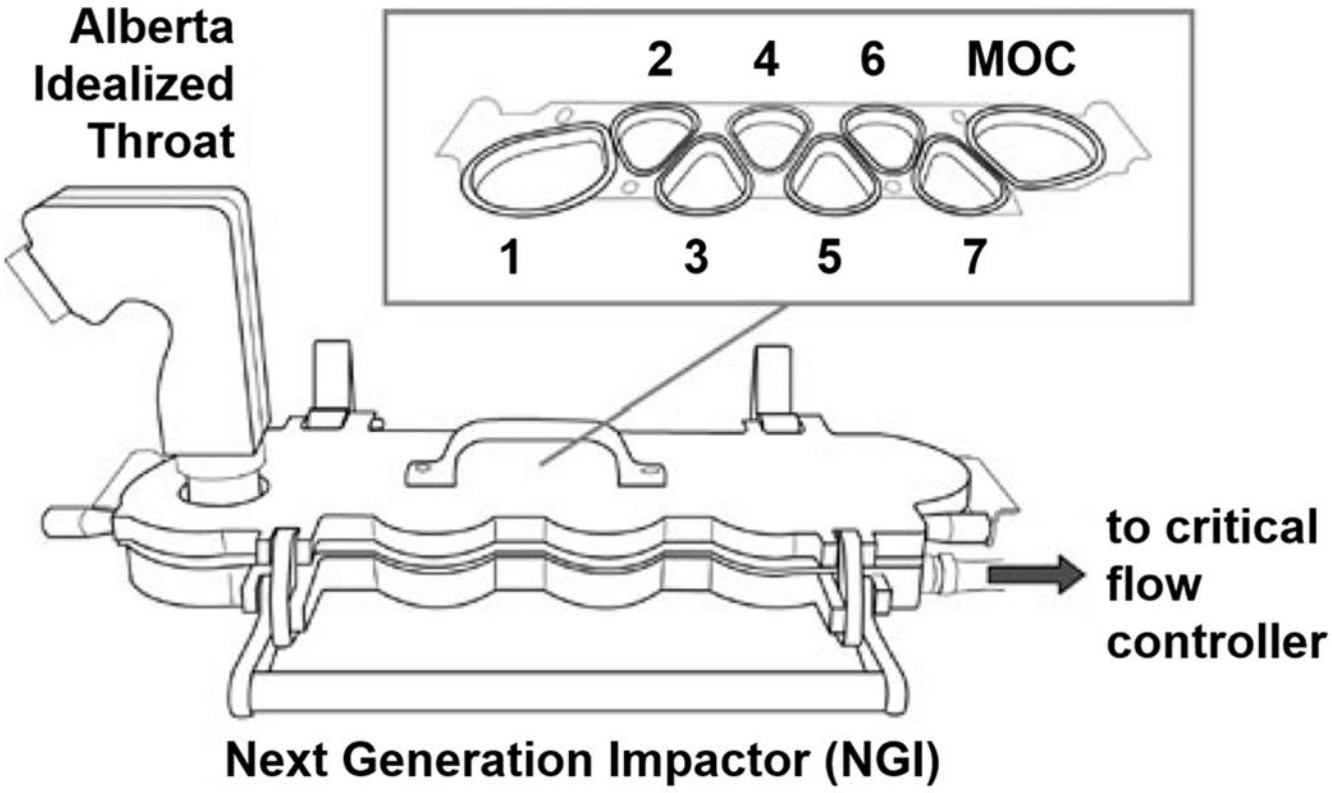

Figure 1.

In vitro aerosol performance testing apparatus [45]. The Alberta Idealized Throat was utilized to obtain a reasonable approximation of vaccine powder deposition in the human oral cavity and pharynx (mouth-throat) region. The Next Generation Impactor consists of seven stages and a micro-orifice collector (MOC) for assessment of particle size distribution.

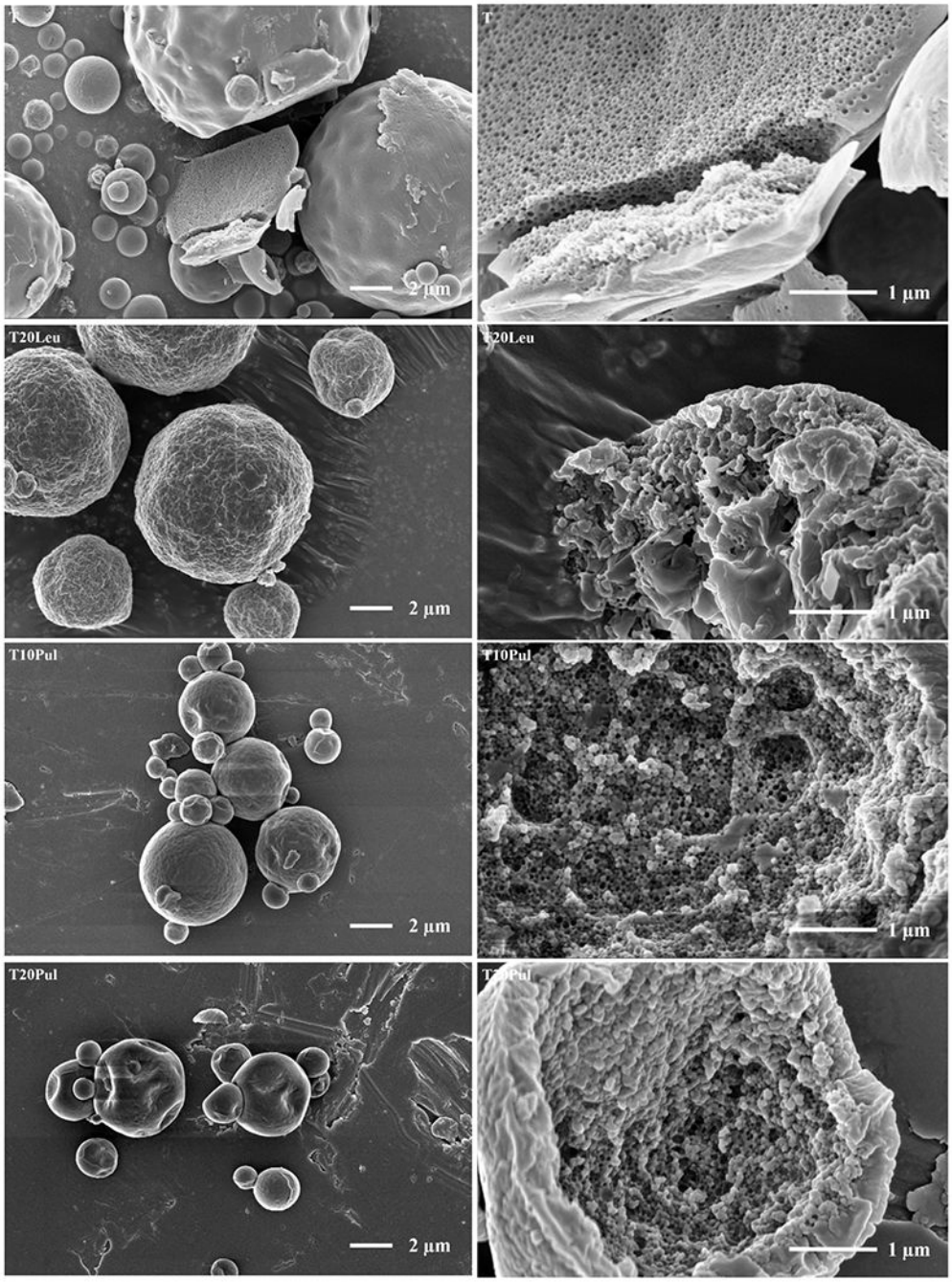

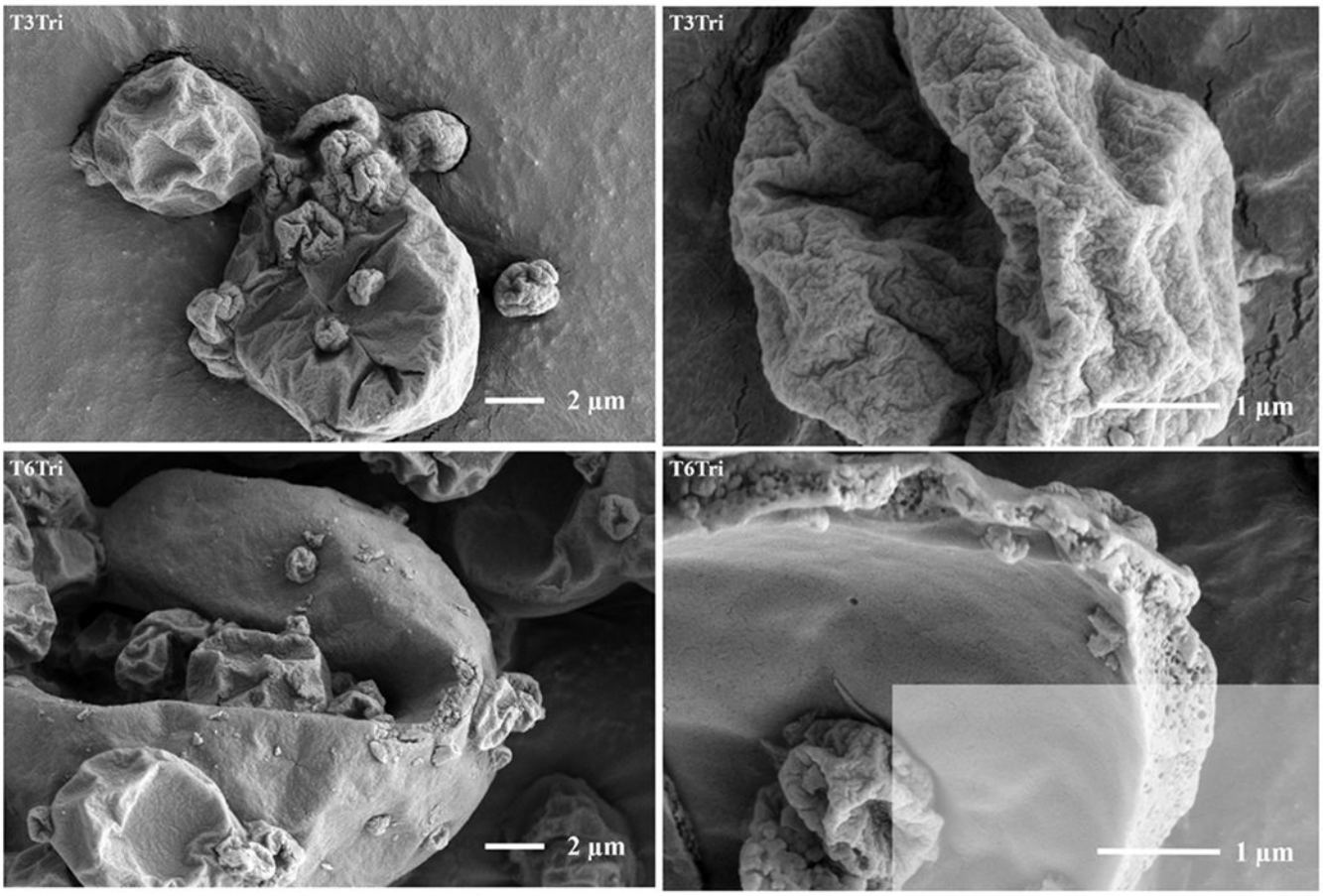

Figure 2.

Low (left) and high (right) magnification SEM images of the inhalable vaccine candidates T, T20Leu, T10Pul, T20Pul, T3Tri, and T6Tri from top to bottom. SEM images showed that exterior particle morphologies vary based on excipient combination. Images of cracked particles indicate the encapsulation of vaccine nanoemulsion droplets. Scale bars are shown on respective images.

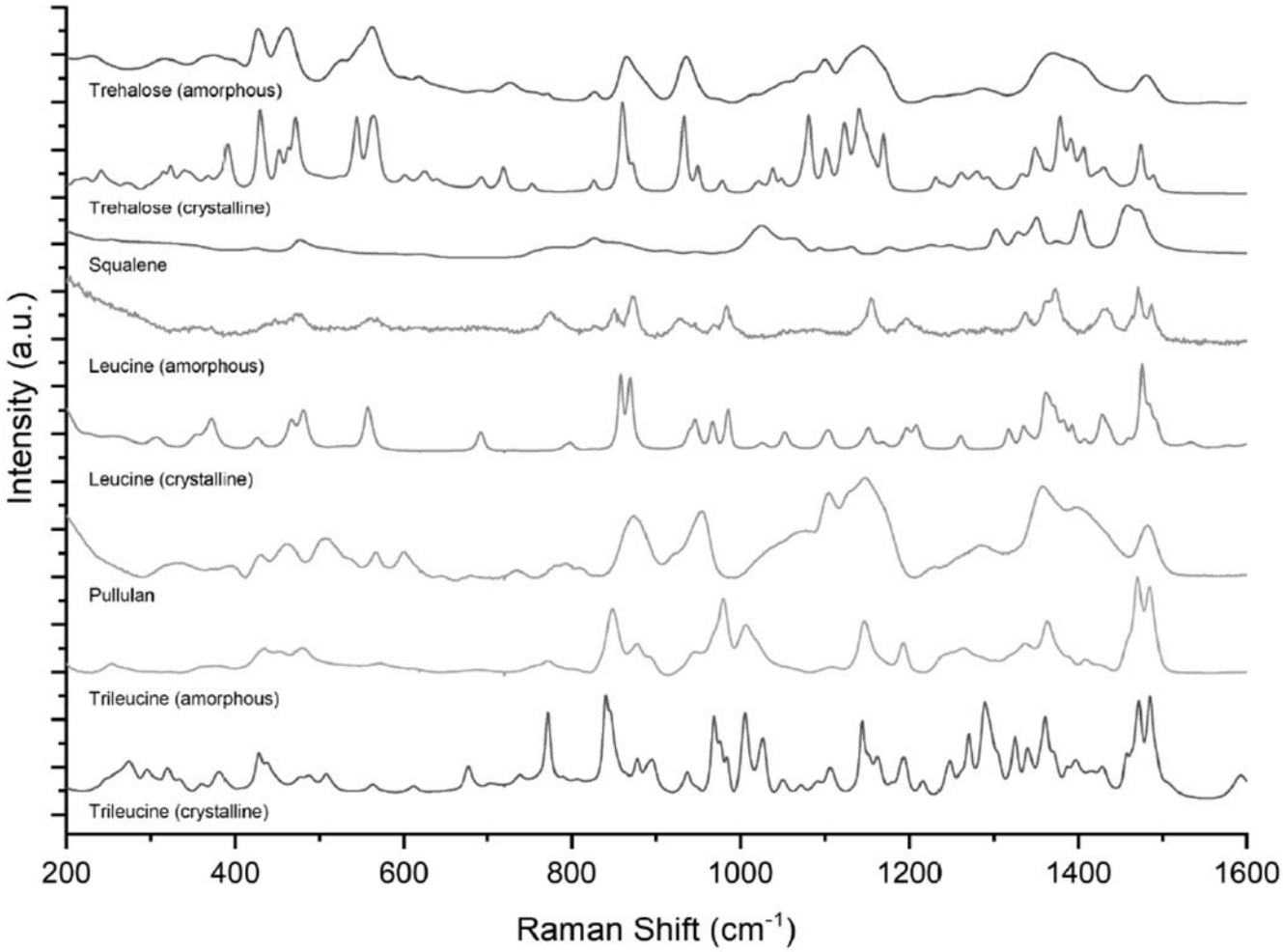

Figure 3.

Reference spectra for the main components of the inhalable vaccine candidates: trehalose, squalene, leucine, pullulan, and trileucine. Amorphous and crystalline reference spectra are shown where applicable.

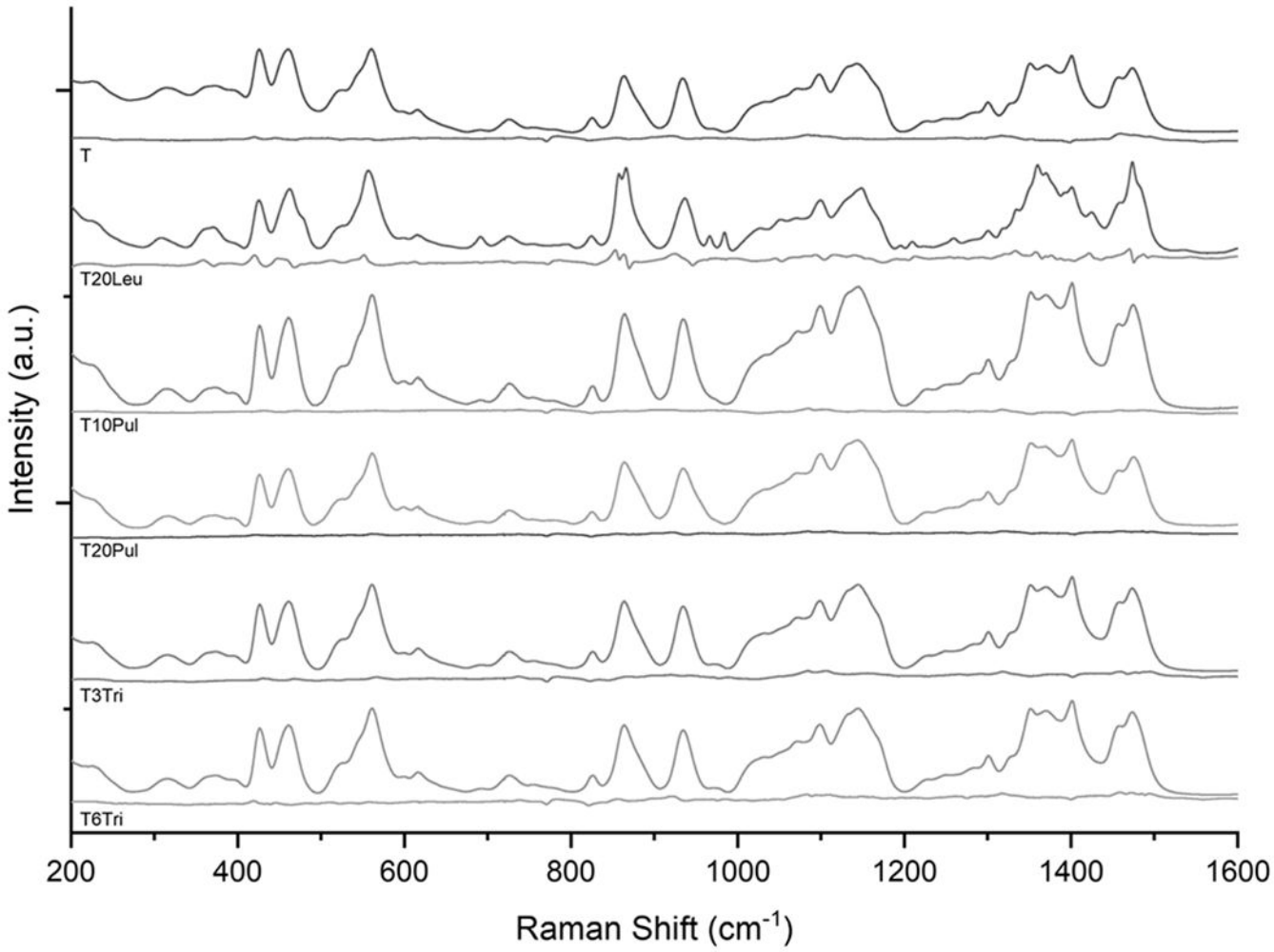

Figure 4.

Raman spectra of spray-dried inhalable vaccine candidates. Respective residual spectra are given underneath the given inhalable candidate sample spectra. Primarily amorphous structure is shown in all candidates, as indicated by the relatively low intensity residual spectra. The leucine-containing T20Leu formulation was the only spectrum that exhibited some crystalline peaks. Peaks shown in the residual spectrum for the T20Leu formulation suggest that the leucine component was mostly crystalline.

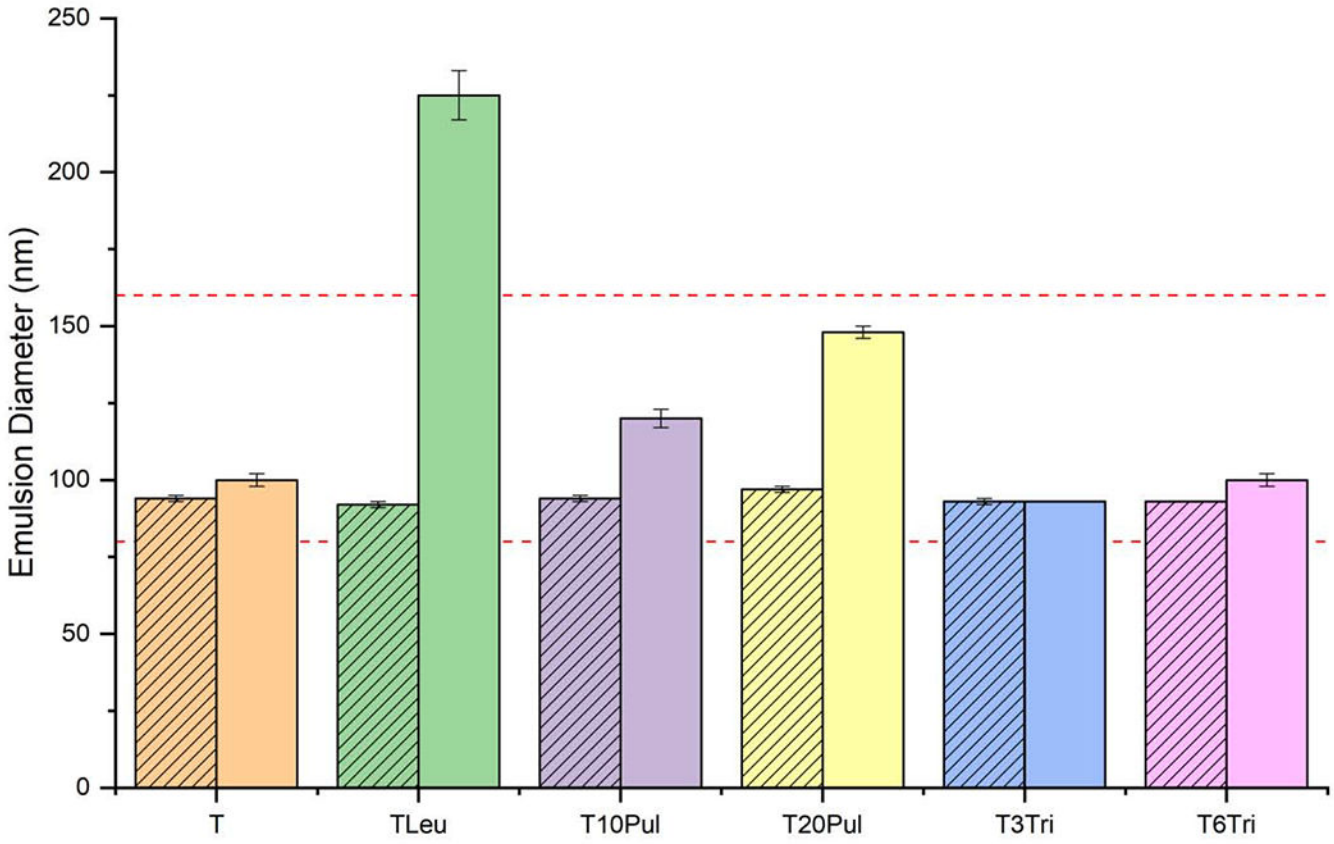

Figure 5.

Droplet diameter of the nanoemulsion before and after spray drying. Addition of pullulan appears to increase the average droplet diameter slightly. Inclusion of leucine greatly increased the droplet diameter. Trehalose-only and trileucine-containing formulations preserved the droplet diameter. Striped bars represent measurements on the liquid feedstock formulations. Solid bars represent measurements on the reconstituted spray-dried powders. Error bars represent the standard deviation of three measurements. Dashed red lines indicate the acceptance limits.

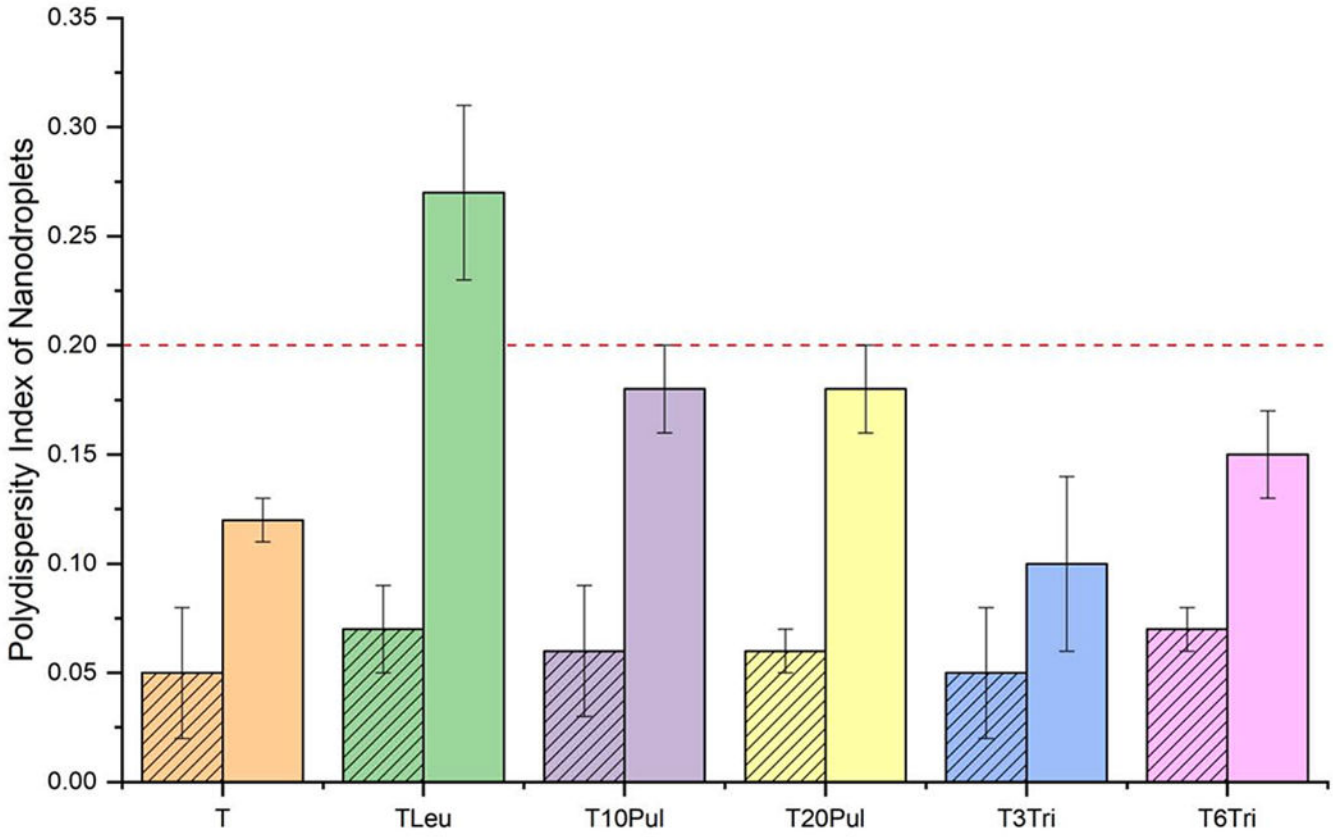

Figure 6.

Polydispersity index of the nanoemulsion droplets before and after spray drying for the inhalable vaccine candidates. The graph indicates that the polydispersity index increased for all formulations after spray drying. The leucine-containing formulation had a polydispersity index greater than 0.2 post-spray drying. Striped bars represent measurements on the liquid feedstock formulations. Solid bars represent measurements on the reconstituted spray-dried powders. Error bars represent the standard deviation of three measurements. Dashed red line indicates the acceptance limit.

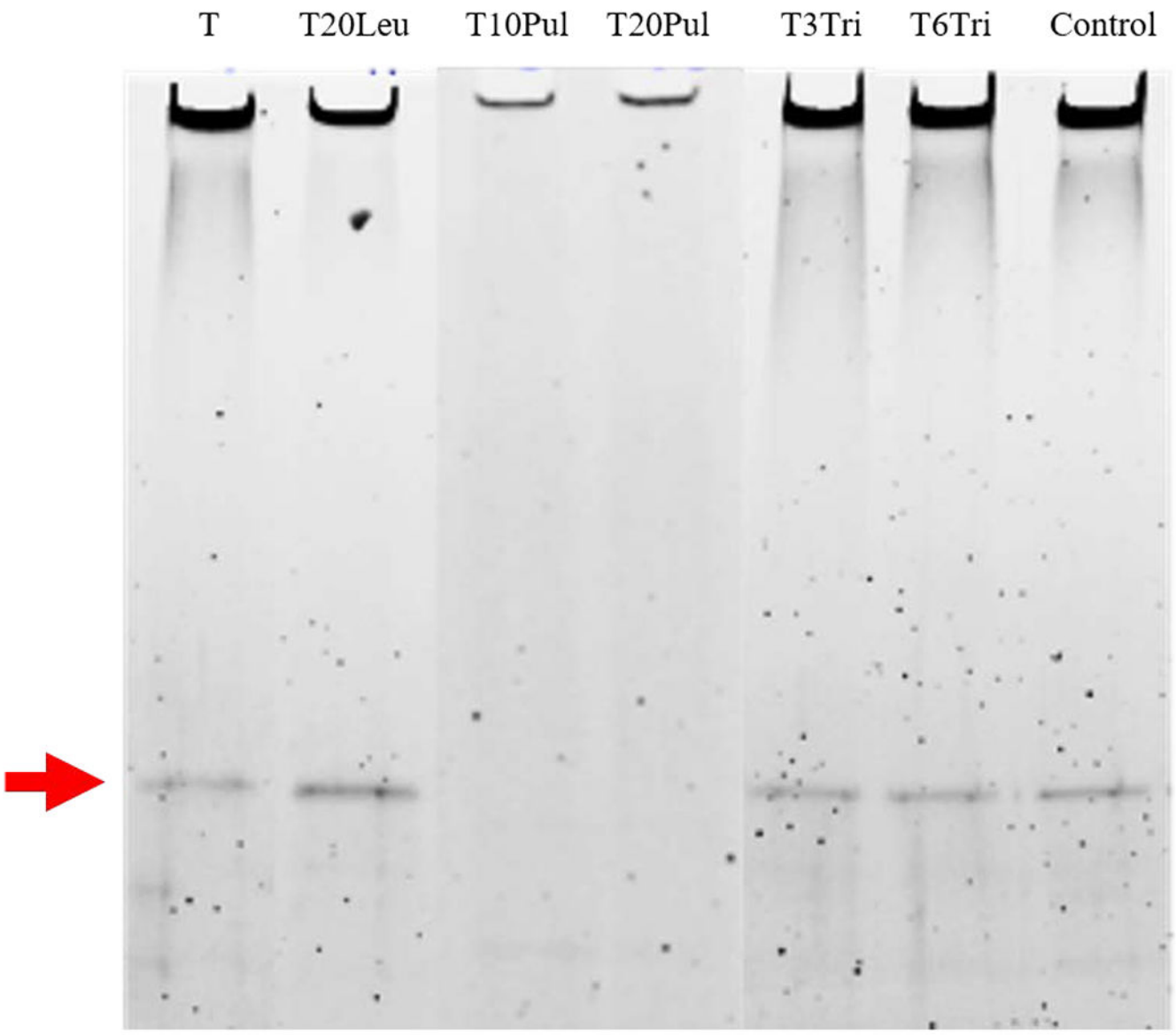

Figure 7.

SDS-PAGE analysis for ID93 presence based on existence and location of band. Analysis was completed on all inhalable vaccine candidates. SDS-PAGE analysis for a control ID93+GLA-SE formulation has been provided in the last lane for comparison. Analysis indicates that the ID93 band is present for all formulations except those containing pullulan. Relative ID93 content among different formulations cannot be determined based on band intensity as the figure shown was combined from different imaged gels.

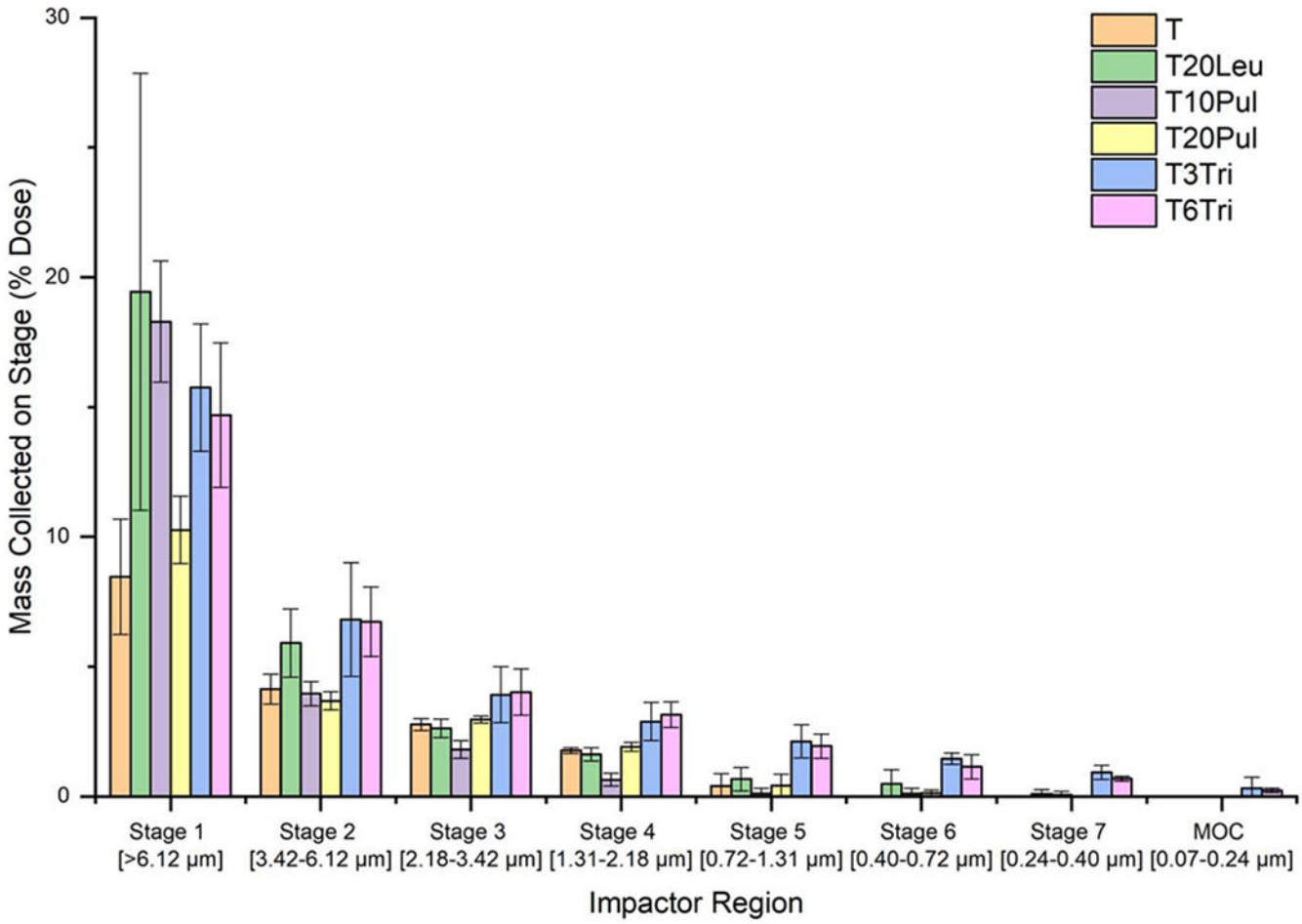

Figure 8.

Mass distribution of the inhalable vaccine powder for each formulation. Depth of penetration varied based on formulation composition. The trileucine-containing formulations had the greatest penetration, with deposition measured on the micro-orifice collector (MOC) of the impactor. Results shown represent the average of triplicate measurements and error bars represent standard deviation.

Table 1

Formulation parameters and designed particle composition by mass of the human inhalable vaccine candidates.

Component\Formulation	T	T20Leu	T10Pul	T20Pul	T3Tri	T6Tri
Feedstock Composition (mg/mL)						
Leucine	-	10.0	-	-	-	-
Pullulan	-	-	4.5	10.5	-	-
Trileucine	-	-	-	-	1.3	2.6
Trehalose	33.3	33.3	33.3	33.3	33.3	33.3
Tris (buffer)	0.807	0.807	0.807	0.807	0.807	0.807
Squalene	5.73	5.73	5.73	5.73	5.73	5.73
DMPC	1.27	1.27	1.27	1.27	1.27	1.27
GLA	0.0033	0.0033	0.0033	0.0033	0.0033	0.0033
ID93	0.0013	0.0013	0.0013	0.0013	0.0013	0.0013
Total Feed Concentration	41.1	51.1	45.6	51.6	42.4	43.7
Particle Composition (w/w)						
Leucine	-	20%	-	-	-	-
Pullulan	-	-	10%	20%	-	-
Trileucine	-	-	-	-	3%	6%
Trehalose	81%	65%	73%	65%	78%	76%
Tris (buffer)	2%	2%	2%	2%	2%	2%
Squalene	14%	11%	12%	11%	14%	13%
DMPC	3%	2%	3%	2%	3%	3%
GLA	0.01%	0.01%	0.01%	0.01%	0.01%	0.01%
ID93	0.003%	0.003%	0.003%	0.003%	0.003%	0.003%

Table 2

Density and solubility values from literature, and calculated *Pe* and E_{SS} for the main components of the spray-dried inhalable vaccine candidates.

Component	Density (kg/m^3)	Solubility (mg/mL)	Pe_i	$E_{ss,i}$	References
Trehalose	1580	690	1.4	1.3	[40], [52]
Leucine	1293	23	0.7	1.1	[56]
Pullulan	1850	Variable	17	6.1	[57], [58]
Trileucine	1250	6.8	1	1.2	[41], [39]
GLA-SE	N/A	N/A	90	30	

Table 3

Feed concentrations of each component, true density, and normalized time for each component to reach true density or saturation for each inhalable vaccine formulation. Abbreviations: tre – trehalose, leu – leucine, pull – pullulan, tri – trileucine.

Formulation	$C_{0,tre}$ (mg/mL)	$C_{0,leu}$ (mg/mL)	$C_{0,pull}$ (mg/mL)	$C_{0,tri}$ (mg/mL)	$\rho_{t,mix}$ (kg/m^3)	$\frac{\tau_{t,tre}}{\tau_D}$	$\frac{\tau_{s,leu}}{\tau_D}$	$\frac{\tau_{t,pull}}{\tau_D}$	$\frac{\tau_{s,tri}}{\tau_D}$
T	33.3	-	-	-	1438	90.3%	-	-	-
T20Leu	33.3	10	-	-	1411	90.2%	37.2%	-	-
T10Pul	33.3	-	4.5	-	1473	90.5%	-	93.0%	-
T20Pul	33.3	-	10.5	-	1510	90.6%	-	87.9%	-
T3Tri	33.3	-	-	1.3	1428	90.3%	-	-	62.3%
T6Tri	33.3	-	-	2.6	1425	90.3%	-	-	40.2%

Table 4

Measured squalene and GLA content before and after spray drying for all inhalable candidates. All values are within 20% of the target.

Formulations	Squalene Concentration (mg/mL)		GLA Concentration (μg/mL)	
	Liquid	Reconstituted Powder	Liquid	Reconstituted Powder
Acceptance Limits	4.58 - 6.88		2.66 – 4.00	
T	6.31 ± 0.12	6.27 ± 0.07	3.72 ± 0.08	3.77 ± 0.00
T20Leu	6.11 ± 0.06	6.35 ± 0.14	3.57 ± 0.02	3.73 ± 0.07
T10Pul	5.71 ± 0.08	6.10 ± 0.07	3.66 ± 0.02	3.77 ± 0.05
T20Pul	5.93 ± 0.07	6.21 ± 0.08	3.73 ± 0.01	3.83 ± 0.02
T3Tri	6.21 ± 0.02	6.42 ± 0.10	3.67 ± 0.02	3.83 ± 0.05
T6Tri	6.37 ± 0.11	6.89 ± 0.07	3.64 ± 0.04	3.52 ± 0.12

Table 5

Emitted dose, lung dose, and particle size analysis of the deposited powder for all inhalable vaccine candidates after aerosol performance experiments. Emitted dose was defined as the mass of powder that has left the DPI, and lung dose was defined as the mass of powder that penetrates the throat model. Both parameters are given as a percentage of the powder dose mass loaded into the capsules. Size distribution parameters $d_{a,50}$ and σ_g were calculated via a fit to the cumulative lognormal distribution of the powder that deposited on the impactor stages. Results shown represent the average of triplicate measurements and error bars represent standard deviation. Statistically significant differences relative to the T formulation are marked with an asterisk. Bracketed values are greater than the Stage 1 cutoff diameter.

Formulation	Emitted Dose (% Dose)	Lung Dose (% Dose)	$d_{a,50}$ (μm)	σ_g
T	87 ± 13	18 ± 0.5	5.7 ± 0.8	2.3 ± 0.1
T20Leu	97 ± 3*	32 ± 12	(8.8 ± 2.3)*	2.9 ± 0.6
T10Pul	89 ± 13	25 ± 3	(10.8 ± 0.3)*	2.5 ± 0.3
T20Pul	84 ± 12	19 ± 2	(6.4 ± 0.2)*	2.6 ± 0.3
T3Tri	93 ± 15	34 ± 6*	5.7 ± 0.2	4.2 ± 1.5
T6Tri	96 ± 6	33 ± 6*	5.4 ± 0.2	3.4 ± 0.4*